JIMMA UNIVERSITY
College of Social Sciences and Humanities
Department of Geography and Environmental Studies

Impacts of Urban Sprawl and Land Use Dynamics on Urban Fringes Agriculture and Land Surface Temperature: The Case of Woliso Area Oromia National Regional State

BY: FIKADU FITESA

A Thesis Submitted to the Geography and Environmental Studies Post-Graduate Program, Jimma University, in Partial Fulfillment of the Requirements for the Award of a MSc. Degree in GIS and Remote Sensing

MAIN ADVISOR:	Dr. GIRMA ALEMU
CO-ADVISOR:	Mr. SOLOMON CHERU
INTERNAL EXAMINER:	Dr. AJAY BABU
EXTERNAL EXAMINER:	Dr. ASNAKE MEKURIA

05-Jun-2023
Jimma, Ethiopia

Declaration

Thesis Submission Request

Name of Student: **Fikadu Fitesa** **ID No. RM 0270/13-0**

Program of Study: **GIS and Remote Sensing - MSc. Program**

Title: Impacts of Urban Sprawl and Land Use Dynamics on Urban Fringes Agriculture and Land Surface Temperature: The Case of Woliso Area Oromia National Regional State.

I have incorporated the valuable comments and suggestion given during the thesis preparation and defense and got the approval of my advisors and examiners.

Name	Signature	Date
Fikadu Fitesa	_____	_____

We, the thesis advisors and examiners have verified that the student has incorporated the suggestion and modification given during the thesis preparation and defense hence the thesis is ready and we recommend it to be submitted.

Name	Signature	Date
Main Advisor: Dr. Girma Alemu	_____	_____
Co-Advisor: Mr. Solomon Cheru	_____	_____
Internal Examiner: Dr. Ajay Babu	_____	_____
External Examiner: Dr. Asnake Mekuria	_____	_____

ACKNOWLEDGMENT

I have great gratitude and appreciation for all those helped me by materials, reading the thesis and providing me valuable suggestions. -- Oh! It has been impossible to realize it without -- Girma Alemu (PhD.) (My adviser) – reading the thesis unconditionally and giving valuable suggestions, giving me his valuable time from his work load; Tsegaye Fitesa - reading and giving valuable suggestions; Worku Fitesa (PhD.) – your core financial and moral supports; Both Mam and Dad – I am here because you are close by;

----------Thank you very much! ----------

Before I go, all my teacher in Jimma University, college of social science and humanities, Department of Geography and Environmental Studies; All my classmate graduate class and Jimma Community 2021 - 2023

---------- all are always memorable! ----------

Table of Contents

List of Tables

List of Figures

List of Annexes

Abstract

This study explored the impact of urban sprawl and land use dynamics on urban fringes agriculture and LST from 1991 to 2021 in Woliso town of Oromia Regional State. The freely accessible Landsat satellite image data collection 2 level 1 (5 TM, 7 ETM$^+$ and 8 OLI/ TIRS) of 1991, 1996, 2001, 2006, 2011, 2016 and 2021 were used. LULC classification result of 1991 showed dominant LULC classes were agricultural land and forest. In 2021 agricultural land, grassland and forest significantly reduced. Conversely built-up and bare land showed drastic increment. The conversions of land from agriculture to built-up represent the most prominent land cover change due to urban sprawl. From 1991 to 2021 about 1186.47 hectares of agricultural land and 100.19 hectares of forest land were converted to built-up area. In contrary only minimal quantity of dry bare lands converted to built-up area showing rapid urbanization was consuming valuable land spaces. More large quantity of agricultural land was converted to eucalyptus tree plantation and ***khat*** *(local name chaat) production showing the spectral reflectance band as forests. The size of total cultivable land significantly affected. The socio-economic impacts posed was more of pressing. The successive spatiotemporal Pattern of NDVI and NDBI also showed generally the presence of LULC transformation. Vegetation cover decreased at stepwise per study years. With the expression (1-NDVI) computed showed the existence of steady increment in built-up and barren land. Spatial distribution of mean LST showed incremental trend of 2.07^{0}C. Gradual increase of LST was found for all land covers over the study period irrespective of land cover type but the LST amplified at elevated rate in areas where the LULC classes were transformed to built-up and bare land. Finally, the regression analysis between LST and NDVI carried out for the selected LULC classes showed that relationship between LST and NDVI has a negative correlation. On the other hand, LST and NDBI showed strong positive linear correlation for all the years. The governmental and non-governmental bodies should give high attention for proper land-use management and socioeconomic effect of LULC change.*

Key Words: - GIS; Remote Sensing; Land use land cover; Land surface temperature; Vegetation indices;

Acronym

ETM+	Enhanced Thematic Mapper Plus
FGD	Focus Group Discussion
GIS	Geographic Information System
KII	Key Informant Interview
LST	Land Surface Temperature
LULC	Land Use Land Cover
MWA	Mono Window Algorithm
NDBaI	Normalized Difference Barren-land Index
NDBI	Normalized Difference Builtup-Area Index
NDVI	Normalized Difference Vegetation Index
NDWI	Normalized Difference Water Index
OLI and TIRS	Operational Land Imagery and Thermal Infra-Red Sensor (TIRS)
PCC	Post Classification Comparison
RS	Remote Sensing
SCA	Single Channel Algorithm
TM	Thematic Mapper
UHI	Urban Heat Index
USGS	United States Geological Survey

CHAPTER ONE

1. INTRODUCTION

1.1. Background to the Study

According to the World Bank, (2011) the world is becoming increasingly urbanized and indeed, half of humanity is now living in urban areas, and more than 70% of the populations of Latin America, North America, and Europe are living in cities. Although 60% of the people in Sub-Saharan Africa still live in rural areas, it is the fastest-urbanizing region of the world (World Bank, 2011). In fact, the United Nations, (2009) predicts that by 2030 Africa will be a predominantly urban continent. At country level Ethiopia is projected to grow from 108 million inhabitants in 2018 to 191 million in 2050 while the urban share is projected to increase from 21% to 39% of the total inhabitants (United Nations, 2019). According to official figures from Ethiopian Central Statistics Agency, the urban population is projected to nearly triple from 15.2 million in 2012 to 42.3 million in 2037, growing at 3.8 % a year.

Urbanization stems in part from rural-to-urban migration, in part from natural increase, and in part from the reclassification of urban boundaries as cities expand outward and small population centers grow and are designated as urban areas (World Bank, 2011). From a socio-economic perspective, cities are considered as magnets that attract people for various social and economic opportunities (Fonseka et al., 2016); Owing to the resource pool and livability attraction, the number of city populations has dramatically increased in the last few decades (Dissanayake, 2020).

Urban growth and urbanization significantly affect different facets of the ecosystem including land, water, ecology, environment and climate system (Ouma et al., 2021). As said by Change and Lanka, (2020) multiple earlier studies have well proven that urbanization is the driving force for changing LULC in city and the intensification of urbanization as characterized by LULC dynamics. The consequences resulting into the diminishing of natural biodiversity and the making of urban warming effects in growing metropolis is of great concern in terms of planning and also as a contributor to climate change (Ouma et al., 2021).

As said by Balew and Korme, (2020) and Zhao et al., (2020) urban areas LULC transformation is a common spectacle mainly the expansion of impervious surfaces like buildings, asphalt

roads etc. These rapid expansion at the expense of other land-cover types like vegetation, wetland and water bodies rise thermal accumulation (Rousta et al., 2018; Balew and Korme, 2020). Hence LULC change detection is a significant factor in the urban study, environmental change, and urban expansion monitoring (Dissanayake, 2020).

1.2. Statement of the Problem

Due to the increase of population, industrialization and other natural and human activities, both urban and rural areas LULC patterns are changing(Wilson and Chakraborty, 2013). In the recent time, global warming and environmental problems are a headache for both within developing and developed countries. Practices like urban sprawl, unplanned land-use for settlement, deforestation, and other activities lead to environment misuse and change.

With related article conducted by Kassa, (2013) in Addis Ababa; Gebregziabher, (2014) in Mekele; Deribew, (2020) in Sebeta-Hawas town; Belay, (2014) in Gondar; Mekuriaw, (2019) in D/Markos; Dessu et al., (2020) in four Southwest Ethiopian urbans; all revealed that rapid conversion of conserved land and cropland to non-agricultural use is threatening the ecological areas and dominant agricultural activities due to urban land use encroachment and urban sprawl as LULC change in respective urban fringes of their study areas.

Woliso area have diverse LULC patterns that has been changing at rapid rate. There has been extensive urban sprawl at urban periphery. It had manifested through squatter settlement on urban fringes agricultural land and legal provision of residential land not supported through smart growth principle. Yet not legally binding land marketing practiced as hedge and land speculation devastate extensive urban sprawl. Additionally, most study shows that rural-urban migration, natural population growth, lack of proper urban housing provision, inefficient and poor urban management and development were major contributors of these conditions. On the other hand, though not supported by research in the study area, LST was assumed to be increasing occasionally in the perception of local communities.

Accordingly, the basic argument this study was proposed and conducted for no similar work piloted on Woliso area, that detects the trend of LULC change, to support prevailing urban sprawl on rural-urban fringes agriculture by empirical evidence, to detect the perception of community if LST of the area was rising, and to analyze the implication and relation of LULC

change on LST. Hence, it was conducted to investigate the level and impacts of urban sprawl on agricultural land resource and compute the trend of LULC transformation, to know the correlation between LST and LULC and to analyze the impact of LULC dynamics on LST change using geo-spatial technologies like GIS, Remote sensing imagery and geo-statistical tools. Therefore, understanding trend of LUL change, urban sprawl as land use dynamics and its level of encroachment on agricultural land resource and their respective implications on land surface temperature could be a guide for planners, decision-makers and citizens who want to create a healthy, affordable and sustainable urban future.

1.3. Objectives of the Study

1.3.1. General Objective

The general objective of the study was to assess impacts of urban sprawl and land use dynamics on urban fringes agriculture and land surface temperature in Woliso town and its surroundings.

1.3.2. Specific Objectives

The specific objective of the study is:

- To assess the trends of urban sprawl and spatio-temporal land use land cover change of Woliso town and its surrounding;
- To evaluate the impacts of urban sprawl and land use dynamics on urban fringes agriculture of Woliso town and its surrounding;
- To assess the implications of urban sprawl and land use dynamics on land surface temperature of Woliso area;

1.4. Research Questions

Understanding the impact of LULC and vegetation on LST could serve to be useful for land management and planning strategies focused on LST mitigation and the adaptation of the study area to the challenges of climate change. All the activities were based on the above general and specific objectives correlated with the following research question.

- What are the spatiotemporal patterns of LULC changes of the study area?
- What is the impact of urban sprawl and LULC dynamics on the surrounding urban fringes agriculture?
- What are the implications of urban sprawl and LULC dynamics on LST of the area?

1.5. Significance of the Study

In Ethiopia in general and in its most emerging urban hubs in particular, where there is poor land information, improving its land administration system has given a great attention currently. In contrary to this there is limited overall local study that conducted to assess the challenges and practices of rapid urban sprawl control, rapid and extensive land use land cover change from productive agriculture to Builtup land use in rural-urban fringes and their implications on LST in Ethiopia. Mainly this is a fact issue in Woliso area yet.

The study hoped that the findings assess and 1) provide necessary information about the trend of LULC and LST Change; 2) provides information about the extent of agricultural land conversion to Builtup area due to extensive urban sprawl and 3) It could be used as an input for policy makers, urban and rural land managers, natural resource managers, environmental experts and other concerned bodies for decision-making related to how LULC and LST change through time. In addition to this, it can be a reference or initial step and use as input for coming researchers based on the analysis of the study. Also, it can help to quantify the relationship between LST and LULC, and can be a vital input to predict future land warming.

1.6. Scope of the Study

This study was delimited geographically, thematically and methodologically. Geographically, the study was conducted on Urban and peri-urban areas of Woliso town. Since the town has been expanding horizontally over time converting lands that were previously under the Rural District, all adjacent rural district has been included as with the Urban expansion, land use pattern has also changed from agricultural use to extensive urban land use purposes.

Thematically, the study concentrated on an impact of urban sprawl as LULC change on farm lands surrounding Woliso towns and respective land use changes to agricultural lands as well as its implication on LST. Operationally, the spatial extent of the study was limited to the thematic mapping and analysis of Woliso town and its surrounding LULC change and LST from 1991 to 2021.The satellite image data for the study covers the 1991, 2006 and 2021 Landsat images for LULC analysis and 1991, 1996, 2001, 2006,2011, 2016 and 2021 for LST. This study used a mixed approach and the methods in the collection of data was stratified random sampling for accuracy assessment.

1.7. Organization of the Study

Generally, the paper comprises five major parts. The first chapter outlines the introduction part, which cover background of the study, statement of the problem, research objectives, research questions, study significance and scope of the study. The second one presents literature review on urban sprawl, trends of urban sprawl in Ethiopia and its causes and consequences, land use land cover (LULC) mapping by image classification, classification accuracy assessment, multitemporal image analysis and change detection, LST, and its retrieval methods. The third focuses and details Methods and Methodology used and followed in the study that comprises description of the study area, types of data and data source, method of data collection tailed and data analysis methods applied including the software packages used, image classification, accuracy assessment, change detection and analysis, LST retrieval from thermal band, NDVI and NDBI calculation. Chapter four presents the detailed results from the analysis with discussion. In this section, results of LULC classification, and LULC Changes, accuracy assessment, LULC dynamics on urban fringes agriculture, spatiotemporal pattern of NDVI and NDBI, spatial and temporal distribution of LST pattern, LULC change and LST link, Correlation between LST and NDVI, Correlation between LST and NDBI presented with discussion. Also, the analysis maps and graphs of LULC, LST, NDVI and NDBI generated for comparison of changes detailed here. Finally, the last chapter presents major findings of the study as conclusions and recommendations. In this section, key findings and critical points that need further treatment were concluded and forwarded as recommendations for decision maker and for future research. The annexes contain data used during the study and a list of key informants.

CHAPTER TWO

2. LITERATURE REVIEW

2.1. Introduction

Review of related literature is crucial and important guide of any research to manage, analyze, interpret, and to draw conclusion and recommendations for the outcome. Hence, this chapter briefly discusses review of related literature to the title of the study. Theoretical and Conceptual Framework from related literature under the sub topic Urban Sprawl, Land Use Land Cover Mapping by Image Classification, Accuracy Assessment, Multitemporal Image Analysis and Change Detection, Multitemporal Map-to-Map Comparisons for Change Detection and Land Surface Temperature has reviewed as follows.

2.2. Urban Sprawl

As a consequence of rapid urban expansion, the occurrence of urban sprawl has allowed the boundary of urban areas to be expanded and to cause significant encroachment on rural areas (Wu, 2008). The concept of urban sprawl can be broadly described as a, "type of uncoordinated development with impacts such as loss of agricultural land, open space and ecologically sensitive habitats in and around urban areas due to lack of integrated and holistic approaches in regional planning,"(Mohan et al., 2011). The consequent impacts of urban sprawl can be viewed from two prominent perspectives; in terms of the encroachment on rural development and in terms of the suburbanization process (Kercival, 2015).

Noted by Rahman, (2016) as earth's population rise and national economies continue to move away from agriculture-based system, cities will grow and spread. Urban sprawl often infringes on viable agricultural or forest land, neither of which can resist or deflect the overwhelming momentum of urbanization (Wilson and Chakraborty, 2013). As stated by Wadduwage et al., (2017) growth spurts of urban populations found a big rise in the housing density within the urban center, thus, this further stimulated the expansion of low-density housing as people sprawled from these city edges, moved from the urban facilities looking for better standard of living and in doing so, began to encroach on the nearby rural areas (Grimm et al., 2008).

As said by Zhao et al., (2020) and Anwar et al., (2021) urbanization leads to the construction of various urban infrastructures in the city area for residency, transportation, industry, and

other purposes, which causes major land use change. It is an indicator of industrialization and generally had an adverse effect on the vegetation by contributing greatly to its depletion, in which the process in-turns intensified the warming of the immediate surroundings (Fabeku et al., 2018).

Expansion of urban area changed the surface radiative properties that imbalanced surface energy, and consequently, affected the LST with an increasing trend mainly due to urbanization; and human thermal discomfort markedly shifted from moderate to strong heat stress (Kemarau and Eboy, 2020; Anwar et al., 2021). They also noted that area of higher temperature zones raised due to expansion of urban areas and bare lands. Moreover it consumes much more land than regular urban developments for zoning laws usually require that new growths are of low density and hence overall density is often sunk by "leap-frog development" (Darrin and Kaminiski, 2016). This term refers the relationship, or lack thereof, among subdivisions which are separated by large green belts, i.e. tracts of undeveloped land, resulting in an average density lower than the low density described (Darrin and Kaminiski, 2016).

The encroachment of urban area on a rural landscape has changed rural communities in terms of their traditional organization, settlements, markets and also soil fertility (Grimm et al., 2008; Wu, 2008). Some studies have highlighted in an extent that some communities have become lost or absorbed in the surrounding urban areas of growth and as a result have abandoned their traditional ways of living, have lost their identity as a population and in turn have become absorbed in the urban area and lifestyle (Wilson and Chakraborty, 2013).

2.3. The Trend of Urban Sprawl in Ethiopia

Ethiopia's urban population share is one of the lowest in the world, well below the Sub-Saharan Africa average of 37% (World Bank, 2015), but due to its large population size, has the most people living in cities and is set to change dramatically increasing (UN-HABITAT, 2008; World Bank, 2015). It is projected to grow from 108 million inhabitants in 2018 to 191 million in 2050 while the urban share is projected to increase from 21% to 39% of the total inhabitants (United Nations, 2019). Majority of the urban population live in small settlements scattered in the country where as a wide definition of urban settlement allows for a total of 925 cities in the country (UN-HABITAT, 2008). Urban is growing not only in population but also in compaction

of cities and land expansion by including or converting peri-urban areas to urban settings where as the trend in the growth of urban populations is likely to continue (Tesfaunegn, 2017).

Kassa, (2013) in his paper showed the situation in Ethiopia highlighting Addis Ababa city regarding both the rate and nature of cities and urban sprawl, high growth rate was seen along main outlets. Similar study by Terfa et al., (2017) in three urban center (Addis Ababa, Adama and Hawasa) showed that Ethiopia has been undergoing rapid urbanization process as seen in many developing countries that unplanned and uncontrolled resulting in scattered urban growth. Study by Gebregziabher, (2014) under the title 'Impact of Urban Sprawl on Livelihood of Fringe Farmers in Mekelle City' revealed that rapid spatial expansion inevitably leads to the encroachment of urban activities to adjacent rural land which result ultimately to urban sprawl. Correspondingly study conducted by Kebebew, Worku and Babu, (2019) in Laga Tafo-Laga Dadi Town indicated major LULC change with agricultural land lost to built-up being the dominant; and an increase in the number of residents, expansion of new developments and LULC change has caused rapid sprawling growth of the town.

2.4. Causes and Consequences of Urban Sprawl

Factors for perceived rises both conurbation and urban sprawl are the fact that the presence of industry, population pressure, landscape and geographic advantage, and infrastructure access(Kassa, 2013). Alike Deribew, (2020) blends of government policy, socioeconomic, demographic dynamics, and biophysical triggers have driven such transformation. Moreover, for Terfa et al., (2017) the main trajectory of constant urban growth was a result of demographic pressure, while the driving force of population growth is migration and natural birth (Mekuriaw, 2019). Rural–urban migration is driven by pull factors that attract people to urban areas and push factors that force them to leave countryside as employment chance and high wages in urban areas are among the key pull factors (REF, 2021). As cited by Kebede, (2021) in (Assefa and Yismaw, 2018) causes of migration include lack of access to agricultural land, scarcity of non-agricultural employ opportunities, early marriage prevalence, rural livelihood shocks from drought, famine, poverty, ethnic conflict, interrupted education, proximity to main roads and high population densities which all are push factors.

On the other hand Gebregziabher, (2014) on his study concluded that the city is, indeed, sprawling into the nearby rural communities due to the uncontrolled and unauthorized

acquisition and occupation of farmlands; a phenomenon that clearly has its roots in the poor land administration practices in Mekele city. With similar generalization a study conducted by Deribew, (2020) Sebeta-Hawas town over the past three decades has experienced severe urban sprawl following lack of proper development control and management.

As consequences of urban sprawl the intensified constraints, following the fast urbanization processes in the country, are unplanned and uncontrolled that resulting in scattered urban growth, loss of farmland, and environmental degradation(Terfa et al., 2017). The study made by Dessu et al., (2020) on long-term urban LULC dynamics and climate change trends in four urban centers of Southwest Ethiopia (Jimma, Bedelle, Bonga, and Sokorru) revealed that a substantial LULC change due to the extensive urban expansion activities. As a result, the built-up areas showed an increasing trend over the last six decades in all urban centers, in contrast to the decline of vegetation, wetland, and cropland because of conversion of lands to built-up and urban expansion (Dessu et al., 2020). Likewise studies conducted by Deribew, (2020) in Addis Ababa, Belay, (2014) in Gondar city, Fitawok et al., (2020) in Bahir Dar City, and Mekuriaw, (2019) in Debere Markos town all revealed that rapid conversion of conserved land and cropland to non-agricultural use is threatening the ecological areas and dominant agricultural activities that are the main sources of livelihood due to urban land use encroachment and urban sprawl in respective urban fringes of their study areas.

Mainly to conclude about urban sprawl as factors of land use dynamics, analyzing agricultural vs. urban land use is important for ensuring that development does not encroach on valuable agricultural land, and to likewise ensure that agriculture is occurring on the most proper land and will not degrade due to improper adjacent growth (Wilson and Chakraborty, 2013; Wadduwage, 2018). With multi-temporal analyses, remote sensing gives a unique view of how cities evolve. Remote sensing methods can be employed to classify types of land use in a practical, economical and repetitive way, over large areas (Wadduwage, 2018).

2.5. Land Use Land Cover Mapping by Image Classification

The terms ‘land cover’ and ‘land use’ are sometimes employed interchangeably, they refer to basically different concepts (Lillesand et al., 2015); as a practical matter, we must consider both together, while also recognizing the distinction between the two (Campbell, 2011). Land use refers to the principal economic enterprises that characterize an area of land: agriculture,

commerce, manufacturing, and residential whereas Land cover indicates physical features that occupy the surface of Earth, like water, forest, and urban structure (Weng, 2008; Jensen, 2015). The pace, magnitude, and scale of human alterations of the Earth's land surface are unprecedented in human history (Jensen, 2015). Hence timely and accurate information on LULC is vital for planning and management activities and considered as a vital element for modeling and understanding the earth as a system (Lillesand et al., 2015) .

Preparation of a LULC map requires that mapped area be subdivided in the discrete parcels, each labeled with a distinct, mutually exclusive, nominal label(Campbell, 2011). That is, it can be mapped by applying classification techniques to digital remote sensing images for pattem recognition(Liu and Mason, 2009). Yet within each broad categories exist a host of different methods that can be applied toward specific imagery; generally, image classification can be accomplished using either supervised or unsupervised techniques. Supervised classification categorizes every image pixel into one of several predefined land-type classes (Jensen, 2015; Thenkabail, 2016c). The process requires several steps and includes selecting the land-type categories, preprocessing, defining training data, automated pixel assignment, and accuracy assessment. Various supervised classification algorithms exist including the maximum-likelihood classifier(Foody, 2010), nearest-neighbor classification, decision tree classifiers, and object-oriented classification(Jensen, 2015; Thenkabail, 2016c).

In contrast, unsupervised classification usually partition the spectral data of an image into feature space with a minimal input from the analyst (Liu and Mason, 2009). Operating under various constraints specified by the user (e.g., number of clusters, spectral and spatial search radius, bands used, and iterations defined), this classification algorithm will search for natural groupings and produce a map of the number of predefined clusters (Liu and Mason, 2016). These clusters can then be assigned to previously defined information classes (e.g., land cover categories) through an iterative process(Canty, 2009; Thenkabail, 2016c).

In practice, most vital factors must be in consideration for applying any of image classification techniques to digital remote sensing image are Selection of appropriate images, Preprocessing, Selection of classification algorithm, selection of training data, and Assignment of spectral classes to information class(Campbell, 2011; Congalton et al., 2017). Success of classification for land cover analysis depends on smart selection of images with respect to season and date.

Accurate registration of image and correction for atmospheric and system errors are also the required initial steps(Richards J, 1999). Equally, Selection of the classification algorithm available and classification procedure should be made (Khorram et al., 2016). Local experience and expertise are likely to be more reliable guide for selection of classification procedure than universal declarations about their execution (Campbell, 2011). Training data Selection is a main process and as each class must wisely examined to be sure that it is denoted by appropriate selection of spectral subclasses to account for variations in spectral appearance due to shadowing, composition (Richards J, 1999; Campbell, 2011).

Spectral class assignment to informational class that must be defined to accurately map an area by digital classification, a key process is the aggregation of spectral class and their assignment to informational classes. Lastly Display and symbolization plays a role. A wide range of colors exists on color displays and the flexibility in their assignment provides unique chance for effective display of land cover information. It is probably sensible to seek some consistency in symbolization of land cover information to permit users quickly grasp the meaning of a specific map/image without detailed checkup of the legend (Campbell, 2011; Thenkabail, 2016a). From the existing classification techniques, the two most commonly used are the Pixel–Based and Object–Based Image Classification techniques.

2.5.1. Pixel – Based Image Classification

Traditional classifiers typically develop a signature by combining the spectra of all training-set pixels from a given feature; and the resulting signature contains the contributions of all materials present in the training-set pixels, ignoring the mixed-pixel problem(Lu and Weng, 2007). The use of pixel-based methods tends to employ techniques that utilize the spectral information that contained within the individual pixel to create the required and relevant land cover classes (Ban, 2016). Since pixel-based method work directly on individual pixel, no segmentation is conducted, with all image objects replaced by pixels during the calculation. Most of the classifiers, such as maximum likelihood, minimum distance, artificial neural network, decision tree, and support vector machine are the major one (Lu and Weng, 2007).

2.5.2. Object – Based Image Classification

Object refers to the homogenous image region with continuous visual clue or consistent semantics, which are often represented as pixel clusters at multiple scales and it essentially

serve as the bridge connecting geographic entities and image elements (He and Weng, 2018). The object-based classification is similar to that of the pixel-based and its associated methods, however the single areas where the object-based classification differs is that the image is not classified by each individual pixel but rather first through the segmentation of all object's combined pixels and then running the classification on those objects (Lillesand et al., 2015; Ban, 2016). Image segmentation and image classification are the two central crucial steps to the object-based one and as a result incorporates spatial neighborhood properties when being considered in the technique (Blaschke, 2010; Simbangala et al., 2015).

These technique has been often adopted in a number of studies with highly successful results ranging from a decrease in the variances found within each class, a more effective classification process especially when using multispectral imagery and the related algorithms were simple and ease to utilize (Duro, 2012; Simbangala et al., 2015). Likewise, studies that have utilized pixel-based one and then compare their results to that of the results generated by the object-based technique have found that the object-based technique outperforms the previous methods, specifically with regards to the overall accuracy of the classification in a variety of environmental and urban settings (Duro, 2012).

2.6. Accuracy Assessment

Accuracy defines "correctness"; it measures the agreement between a standard assumed to be correct and a classified image of unknown quality. If the image classification agrees closely with the standard, it is said to be "accurate" (Thenkabail and Lyon, 2009; Campbell, 2011). Accuracy assessment task can be defined as one of comparing two sources of information, one based on analysis of remotely sensed data (the map) and another based on a different source of information, assumed to be accurate, the reference data (Lu et al., 2004; Lunetta and Lyon, 2004; Campbell, 2011). To assess accuracy of a map, the map and reference data must be co-registered, that both use the same classification system and minimum mapping unit as they have been classified at comparable level of detail (Lu et al., 2004; Olofsson et al., 2014).

The standard form for reporting site-specific error is the error matrix (Lu et al., 2004), sometimes called the confusion matrix (Liu and Mason, 2009) as it identifies not only overall errors for each class but also misclassifications (due to confusion between classes) by class. Compilation of an error matrix is required for any serious study of accuracy (Foody, 2010;

Campbell, 2011). To construct the error matrix, the analyst must compare two source of data-the reference samples and the classified image-on a point-by-point basis to determine exactly how each of the validation samples is denoted in the classification. It is very essential that the validation samples and the map be well co-registered to one another. Errors in registration will appear as errors in classification, so registration problems will create errors in the assessment of accuracy. This is also true with respect to timing; the validation data and the image should be acquired as close in time as possible (Foody, 2010; Olofsson et al., 2014).

2.7. Multitemporal Image Analysis and Change Detection

Change detection (CD) using remote sensing data is an attempt to record natural and manmade transitions of LULC on Earth's surface that have occurred over time. It involves the application of multi-temporal datasets to quantitatively analyze the temporal effects of the phenomenon (Singh, 1989). It is the analysis of information about a location over two or more points in time and it compares differences in spectral responses of multitemporal imagery captured over the same area. The basic assumption is areas where map classes have remained constant will be denoted by little/no spectral change, and that change will cause spectral variances (Congalton et al., 2017).

Urban area applications of CD has shifted from basic one to the analysis of processes and patterns of urban expansion, measurement of patterns, and quantification of Land use change (Pradhan, 2017). Timely and accurate CD of surface features provide the basis for better understanding relationship and interaction between human and natural spectacles to better manage and use resources (Singh, 1989; Weng, 2008).

For CD it is vital to account for the compatibility of all datasets and future data continuity and availability of remote sensing data in choosing datasets (Khorram et al., 2016). Ideally, it should involve data acquired by similar sensor, the same spatial and radiometric resolution, viewing geometry, spectral bands, and time of day (Lillesand et al., 2015); To detect changes at time scales greater than a year, anniversary dates are ideal to minimize sun angle and seasonal variances (Jensen, 2015). Accurate spatial registration of various dates of imagery is also a must for effective detection (Canty, 2014). The reliability of change detection path may strongly influenced by various environmental factors that might change between image dates (Jensen, 2015). Also factors as water level, tidal stage, wind, or soil moisture condition might

also be important; influences as different planting dates and season-to-season changes in plant phenology must be considered (Lu et al., 2004).

The goal of CD include Detecting change/no-change; Measuring the extent and magnitude of change; Updating existing map or GIS layers to incorporate change; Identifying the causes of change; and Assessing impacts of change on environmental, economic, and political conditions (Lu et al., 2004; Thenkabail, 2016b). To do so it requires development of a classification scheme that clearly define type of change to detected and mapped; capturing variation between dates of imagery/maps related to the change of interest; and controlling all no-change variation among the various dates of imagery/maps to be compared in CD analysis (Lu et al., 2004).

Of many types of CD method that most commonly used by scholars is the Post Classification Comparison (PCC). PCC uses a 'pixel-by-pixel' comparison so as to detect areas of LULC changes. It enables the process of comparative analysis of satellite imagery obtained in a time series to occur after the previous independent classification (Dissanayake, 2020). PCC was identified as the only CD technique that allowed for classes to be calculated based on how each pixel changed from each of the relevant classes. Also, it enables to easily identify previously unnoticeable changes; provide information on the type of changes that have occurred in each class and compensates for majority of the environmental and atmospheric conditions that happen between the two dates in question (Kercival, 2015).

On the other hand spatial scale and information content of satellite-derived remote sensing data has inspired the development of automated CD algorithms and methodologies, especially for evaluating and recording LULC change (Khorram et al., 2016). These methods are categorized as pre-classification and post-classification CD approach. Pre-classifications are primarily armed to identify either binary or scaled indicators of *"change"* or *"no change"* whereas post-classification CD can mostly provide detailed matrix of 'from–to' change and requires a great deal of preparatory analyst input (Khorram et al., 2016).

In automated post-classification CD, the original study imagery (image dates 1 and 2, or more) is thematically classified. The change analysis arises when classified maps are compared by one or more other thematically classified map. Along with the profit of the '*from-to'* output generated by_this approach, it minimizes the effect of atmospheric and environmental gap between input images. In addition, computational simplicity has made this type of analysis a

very popular procedure in comparison to the pre-classification methods (Jensen, 2014). Yet, it is vital to be aware of each classification input introduces error into the post-classification change analysis, and this error is magnified in final change map by the aggregate classification error from each input image (Khorram et al., 2016).

2.8. Land Surface Temperature (LST)

Land surface temperature (LST) is the direct driving element in the exchange of longwave radiation and turbulent heat fluxes at surface-atmosphere interface (García-Santos, 2018). For Jeevalakshmi, (2017) it is the surface temperature which can be measured when the surface is in direct contact to the measuring instrument, and is nothing but the skin temperature of land surface. It is the direct driving factor for water heat exchange between Earth's surface and atmosphere (Rozenstein et al., 2014; Wang, Lu and Yao, 2019).

LST variation in space and time, measured by satellite remote sensing, are used for the estimation of a multitude of geophysical variables, and hence is the key parameter in many physical processes of different surfaces at several scales like global climate change studies, urban LULC, geo-/biophysical (Friedel, 2012; Maimaitiyiming et al., 2014; Jeevalakshmi, 2017) hydrological and agro processes (Avdan and Jovanovska, 2016); soil moisture estimation, in climatic, ecological and biogeochemical studies (Du et al., 2015), urban climate, the hydrological cycle, and vegetation monitoring (Chapin et al., 2005; Kalnay and Cai, 2013; Rozenstein et al., 2014), and also a key input to analyze tendencies toward urbanization and desertification(Mallick, Kant and Bharath, 2008), drought monitoring, are based on spaceborne-derived relationships between LST and the normalized difference vegetation index (NDVI) (Karnieli et al., 2009).

Satellite products offer larger spatial coverage of in-situ measurement, which mainly sparse in certain geographical region (Kuenzer and Dech, 2013). Now the two satellite platform series providing high-resolution LSTs -Landsat and ASTER (Dodd, Veal and Ghent, 2016).

2.9. Land Surface Temperature Retrieval

Since many applications in climatological, hydrological, ecological, and biogeochemical studies rely on the knowledge of LST it is critical to have access to accurate estimates of LST (Wang, Lu and Yao, 2019). Retrieving LST from thermal infrared remote sensing data at

global, regional, and urban scales have matchless advantage, and is the most common method for studying urban heat island effects (Wang, Lu and Yao, 2019).

Accordingly many scholars have studied several algorithms for LST retrieval and they can be roughly grouped into three categories that widely used: the mono-window algorithm (MWA), developed by Qin, Karnieli and Berliner (Qin et al., 2001), the split window algorithm (SWA), developed by Larry M. Mcmillin (Mcmillin, 1975), and the single-channel algorithm (SCA), developed by Jiménez-Muñoz and Sobrino et al. (Jimenez-Munoz et al., 2004). The three algorithms were proposed for the thermal infrared remote sensing retrieval including Landsat platforms (Landsat 5 to 7) with the Thematic Mapper (TM), Enhanced Thematic Mapper (ETM) and Enhanced Thematic Mapper + (ETM+) instruments on board provide LSTs with 90-120m spatial resolution derived from TM, ETM and ETM^{+} IR channels.

Landsat 8 carries two main sensors: Operational Land Imager (OLI) and Thermal Infrared Sensor (TIRS). Though Landsat 8-TIRS contains two thermal infrared bands, band 10 and band 11, which enable the split window algorithm to be used, it was observed for the Landsat 8-TIRS bands that radiance from outside of the instrument's field-of-view produced a non-uniform flash signal across the focal plane that varied depending on the out-of-scene content (Wang, Lu and Yao, 2019). Because of large calibration uncertainty, the USGS does not recommend use of band 11 for the split window algorithm. Though proposed correction algorithm named the stray light correction algorithm (SLCA) to reduce error caused by stray light and has been implemented into the USGS, the Landsat team still does not recommend the use of band 11 for the split window algorithm, because, whether this correction is accurate, it requires more research to prove (García-Santos, 2018; Wang, Lu and Yao, 2019).

Henceforth by way of the three algorithms (MWA, SWA and SCA) were originally proposed for other thermal infrared remote sensing; when applied to Landsat 8 TIR data, they should be improved. And hence Wang et al. (Wang et al., 2015) proposed an improved mono-window (IMW) algorithm based on Qin's MWA, which makes the MWA appropriate for Landsat 8. Rozenstein et al. (Rozenstein et al., 2014) improved the SWA and derived LST from Landsat 8 TIR data and for the SCA method, Jiménez-Muñoz and Sobrino (Jiménez-muñoz et al., 2014) made an improvement for Landsat 8 in 2014.

On the other hand Bonafoni and Sekertekin, (2020) evaluated three NDVI-based LSE models, namely, Sobrino et al.'s, Valor & Caselles' and Van De Griend & Owe's LSE model with toolset developed by **Walawender, Hajto and Iwaniuk**, *'a new ArcGIS toolset for automated mapping of LST with the use of LANDSAT satellite data* (Walawender, Hajto and Iwaniuk, 2012)', were considered for Landsat 5 TM and 7 ETM+ data to investigate their effects on LST methods. Their obtained result showed that Sobrino et al.'s LSE model provides best performance to extract LST for all Landsat missions and LST methods.

CHAPTER THREE

3. METHODS AND METHODOLOGY

3.1. Description of the Study Area

3.1.1. Location

Woliso Town and adjacent rural district areas is one of the districts confined in Oromia National Regional State. The town is the administrative centre of South West Shoa Zone and one of the self-administering urbans of the region. It is positioned at 114 km in south west from capital Addis Ababa and 40 kilometres to the north from Wolkite town of Gurage zone in Southern Regional State of Ethiopia on the main way to the Capital. With approximation total area of the Town and its surrounding rural districts is about 30,504.3 hectare. The latitude and longitude of the area are 8°32'26.76"N and 37°58'21.85"E, respectively and the altitude ranges from 1940 m to 2780 m above MSL (Contour map of woliso area and its surroundings district was attached as annex 3 in appendices part of this paper).

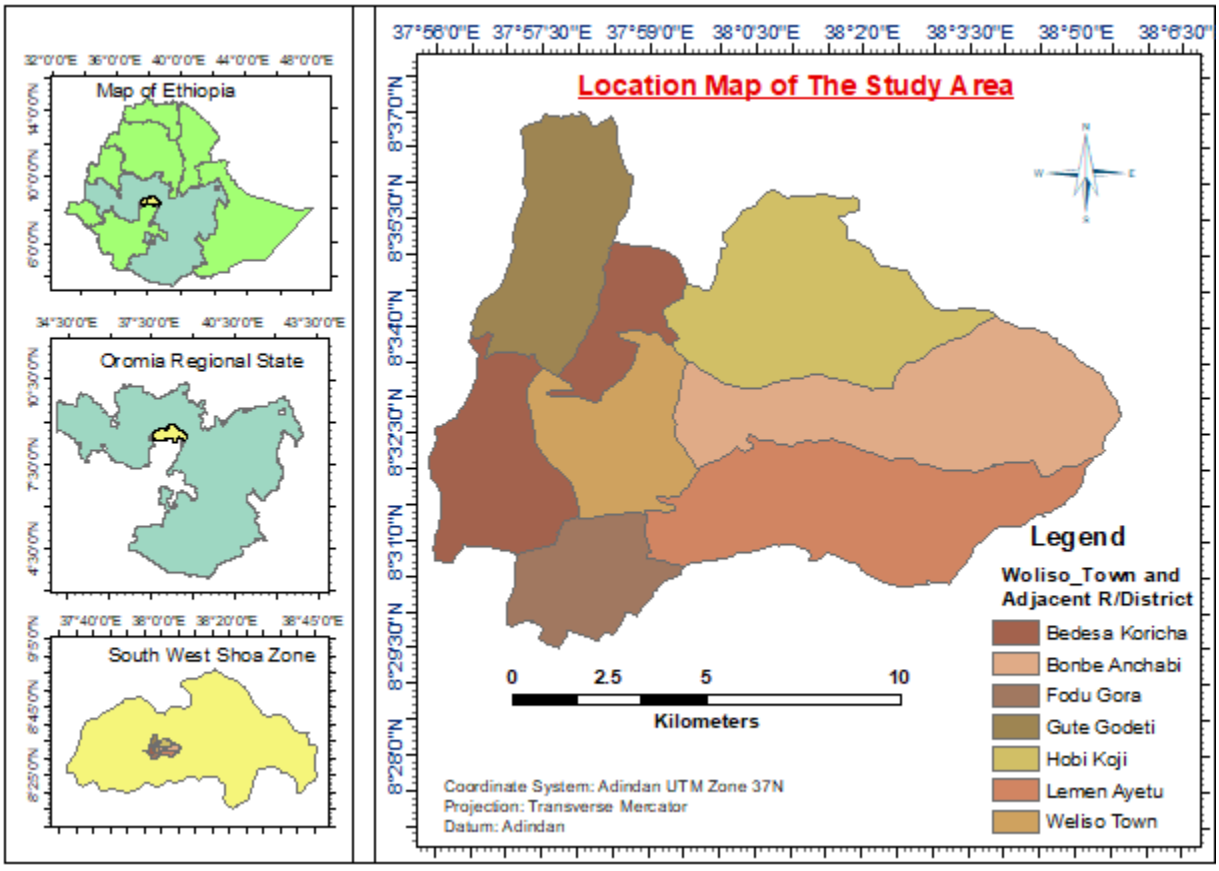

Figure 1: Location Maps of the study area

3.1.2. Topography

Woliso area has a broad flat land. However, in its northwest and east part there are relatively uneven topography. It is bordered on the north by Becho, west by Wonchi, south by Goro, at the East by sadden-Sodo Districts where as in south east by Southern Region of Ethiopia. Walga, and Rebu are the important river in the area. Vegetation distribution is typical and that found in the area are forest and shrubs, Acacia and scattered trees of Eucalyptus which is, grown by local communities. Digital elevation map of Woliso area and its surrounding districts was attached as figure 2 below.

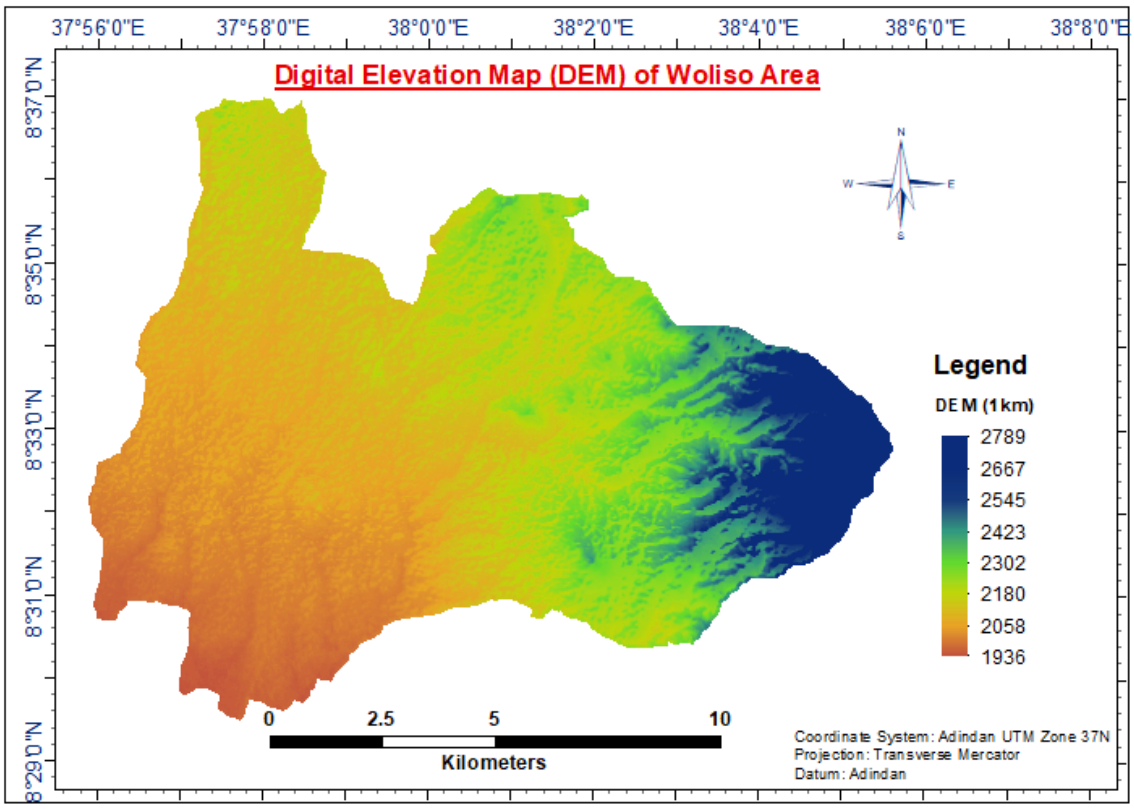

Figure 2: Digital Elevation Map of Woliso area and its surrounding districts

3.1.3. Population and Economy

According to the projected population data (CSA, 2022), the total human population of Woliso Town is 78,577 and all Woliso rural district 202,219 with sum up 280,796. Out of this, 141,605 are women and 139,191 are men. The main economic base and activities are crop production from the highly productive surrounding area farmer associations, livestock farming and commerce. The economy of the town and its residents are mainly based on trades, service provision, crafts and manufacturing. Additionally, there are also urban agriculture to some

extent and others. Data from the municipality viewed illustrates Woliso town has visioned and set goal as agro-industry as well as conference and tourism-based development plan economically and working towards it.

3.1.4. Climate

The document data in the municipality showed that the climatic condition of the Woliso area is characterized as tropical and four main climatic conditions, such as Autumn (September–November), winter which is the dry season (December–February), Spring (March–May), and summer which is highly rainy time (June–August) seasons, are predominantly observed over the study area. The town has metrological station, and hence the document data viewed from the station showed an average annual rainfall of 1,235.2mm which varies with seasons with average annual temperature of 17.8 °C.

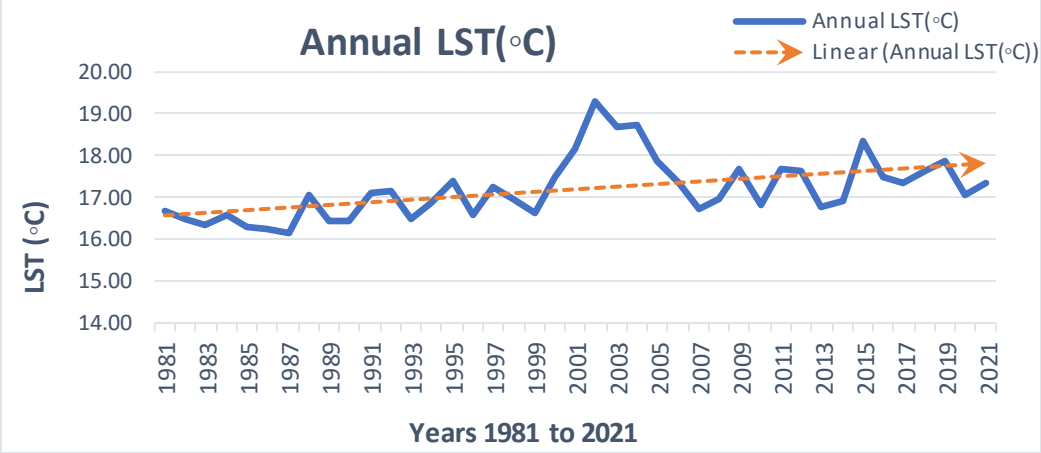

Figure 3:Annual temperature graph of Woliso area (https://power.larc.nasa.gov/data-access-viewer/)

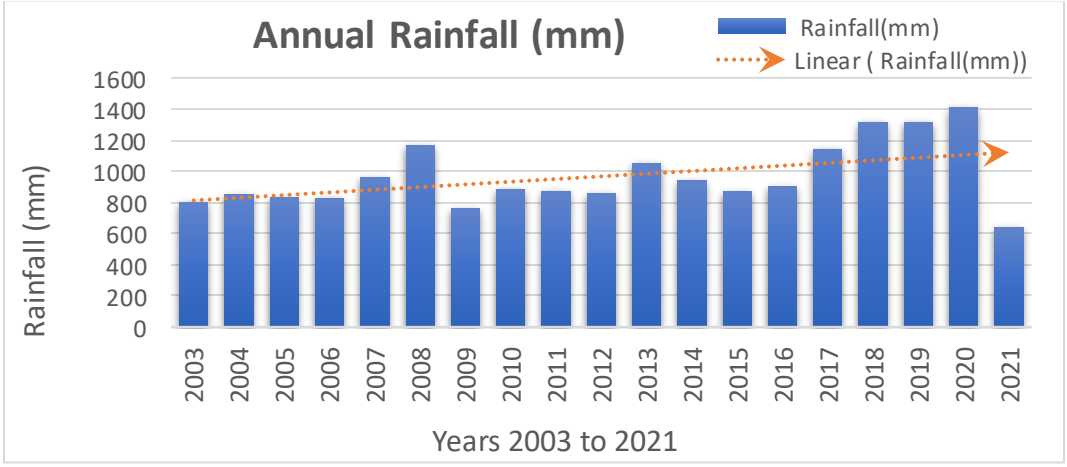

Figure 4: Rainfall graph of Woliso area (https://chrsdata.eng.uci.edu/)

3.2. Types of Data and Data Source

Data used for this research encompasses both primary and secondary (Ancillary) data. The most important source was the primary data (satellite data). The best places to look for remote sensing data and various remote sensing derived products is at the United States Geological Survey's (USGS) *Earth-Explorer* website. Accordingly, the freely accessible Landsat satellite image data the best suitable collection two level one was used. Thus, Landsat image data for the years 1991, 1996, 2001, 2006, 2011, 2016 and 2021 were obtained from the USGS official website (http://www.earthexplorer.usgs.gov/) in a cloud-free condition based on availability.

The satellite image data acquired was used for all including LULC analysis, for change detection and LST evaluation. The 1991, 2006 and 2021 accessed image data was used for LULC classification and change detection analysis, whereas all the accessed Landsat satellite image data was used for all LST retrieval and analysis, NDVI, NDBI calculations and for the correlation analysis. Table 1 below shows the Landsat TM/OLI/TIRS image data used in the study. All the specification of Landsat image bands used in the is attached as annex 1.

Table 1: Landsat TM/ ETM^{+}/ OLI/TIRS images used in the study

Year	Landsat TM/OLI/TIRS image data
1991	LT05_L1TP_169054_19911212_20200914_02_T1
1996	LT05_L1TP_169054_19961209_20200910_02_T1
2001	LT05_L1TP_169054_20011223_20200905_02_T1
2006	LE07_L1TP_169054_20061127_20200913_02_T1
2011	LE07_L1TP_169054_20111227_20200909_02_T1
2016	LC08_L1TP_169054_20161216_20200905_02_T1
2021	LC08_L1TP_169054_20211214_20211222_02_T1

Besides, Sentinel-2 satellite image (10-m spatial resolution) of 2021 with zero cloud cover and Google Earth platform data (5-m spatial resolution) was accessed and used to validate the Landsat land cover data which is with 30-m spatial resolution.

On the other hand, to evaluate the impacts of urban sprawl and land use dynamics on urban fringes agriculture; socio-economic data was used. Governmental institutions like Agricultural office; Rural Land Administration and Urban Land Management offices as well as three rural district agricultural extension Experts and eleven purposively selected household residents

were joined considered. Finally ancillary source of data was accessed from governmental and non-governmental body and published information.

3.3. Method of Data Collection

To accomplish the specific objectives of the study, the socio-economic data was collected through the data collection tools like questionnaires, key informant interview and focus group discussion (FGD). Concerning sampling methods and sample size, since agricultural farm holders that reclassified to urban district were presumed homogeneous and believed that they can provide enough information; the non-probability sampling technique was used. Henceforth focus group discussion body and key informants were purposively selected as the sampling units for this study were households and institutions.

Accordingly, the study applied both qualitative and quantitative data collected from primary and secondary sources. Qualitative data were produced over FGD (i.e., composed of eleven household heads: (eight male and three female) selected purposively from those reclassified to urban district. The choices were done based on the households' age where elderly preferred (i.e., those who lived many years in the area). These data were gathered with the assistance of Extension Worker and district management officials.

The discussions covered precise areas such as the comparison between the size of farmland and the income obtained from farming before and after the urban expansion; whether inhabitants were consulted before expropriation process of the land and other properties; as well as employment opportunities. Also, individual farmland owners were also identified in the study area with the help of Extension Worker and eight informants; two from the four districts were purposively selected for an interview related to the opportunities and challenges that resulted from urban expansion across their areas. Further, Extension Workers were also sources of qualitative information so as to complement information obtained from farmers.

Quantitative data on the number, area and type of LULC classes and LULC change were obtained through Landsat satellite image classification and conversion, LST, NDVI and NDBI retrieval via geospatial analysis tools. Field verifications for the status of the converted lands and the patterns of urban expansions were applied between November and December 2021. Three focal people from the Agricultural office, Rural Land Administration Unit and the Urban Land Management were also selected for the interview.

3.4. Data Analysis

3.4.1. The software packages used

The software packages used for this study were a GIS tools used to work with maps; ArcGIS 10.8, for image analysis like LULC classification, change detection; LST, NDVI and NDBI retrieval, and map preparation; ERDAS IMAGINE 15 to process image enhancement and preprocessing; Microsoft Excel and the open-source software R-4.2.2 were used for statistical analysis charting and plotting.

3.4.2. Image Classification

Supervised classification by utilizing the maximum likelihood algorithm was tailed in this study to classify land cover from Landsat 5 TM, Landsat 7 ETM plus and Landsat 8 OLI/ TIRS data for signature extraction. Accordingly, a sufficient number of signatures were collected from composite band images using google earth imagery, ancillary information and field visit. After merging signatures of the same class, the Maximum-Likelihood method was applied for all the land cover classes. The known land cover was defined and the cell signature value developed for each land cover type. Hence built-up area, vegetation cover, Agriculture, Grassland and Bare-land were chosen as major land covers of the county. The details of five major land cover observed and defined was enlisted in Table 2 below.

Table 2: Major land cover for the study area adopted with modification from U.S. Geological Survey LULC Classification System for Use with Remote Sensor Data.

LULC class	Description
Agricultural land	All cultivated and uncultivated agricultural lands areas such as farmlands, crop fields including fallow lands/plots and Horticultural lands.
Built-up area	Residential, commercial and services, industrial, socio-economic infrastructure and mixed urban and other urban, transportation, roads.
Forest Land	Protected forests, plantations, deciduous forest, mixed forest lands and forest on customary land.
Bare Land	sand dunes, exposed rocks, stripe mines, queries and gravel pits/non-vegetated area dominated by rock out crops, roads, eroded and degraded lands.
Wet Grass land	Permanent and seasonal grasslands along the lake, river and streams, marshy land and swamps, protected communal grass lands

3.4.3. Accuracy Assessment (AA)

The classified maps was assessed on accuracy by stratified random sampling methods (Foody, 2010; Olofsson *et al.*, 2014) since stratified random sampling is suggested where a minimum number of samples are selected from each stratum, and a generally accepted rule of thumb is to use a minimum of 50 samples for each land class category in the error matrix (Indira Gandhi, 2012). Hence, from each LULC class, a typical sample was chosen. Apart from field checked LULC maps, a field survey and google earth imagery derived points saved as kml file was used as reference data. And the error matrix developed and the Over-All-Accuracy; Producers-Accuracy; Users-Accuracy; and Kappa-Coefficient were computed for classification of LULC for the years 1991, 2006 and 2021 consequently. The equations used to compute were:

$$\text{Users Accuracy} = \frac{\text{number of Correctly Classified pixels in each Category}}{\text{Total number of classified pixels in that category (the Row Total)}},$$

$$\text{Producers Accuracy} = \frac{\text{number of Correctly Classified pixels in each Category}}{\text{Total number of Reference pixels in that category (the Column Total)}},$$

$$\text{Over all Accuracy} = \frac{\text{Total number of Correctly Classified pixels (Diagonal)}}{\text{Total number of Reference pixels}}$$

$$\text{Kappa Coefficient} = \frac{(TS * TCS) - \Sigma(\text{Column Total} * \text{Row Total})}{TS2 - \Sigma(\text{Column Total} - \text{Row Total})}$$

Where TS = Total Samples; TCS = Total Correctly Sampled; Σ = Summations

Table 3: Sample-based error matrix where there are k classes in the remote sensing–derived thematic map and N ground reference test samples that are used to assess its accuracy. (Jensen, 2015).

	Class Name	Ground Reference Test Information Class 1 to k (j columns)					Row total xi+	User's accuracy (%)
		LULC 1	LULC 2	LULC 3	…	LULC k		
Map Class 1 to k (i rows)	**LULC 1**	X1,1	X1,2	X1,3	…	X1, k	X1+	X1,1/X1+
	LULC 2	X2,1	X2,2	X2,3	…	X2, k	X2+	X2,2/X2+
	LULC 3	X3,1	X3,2	**X3,3**	…	X3, k	X3+	X3,3/X3+
	.	.	.	.	.	.	.	.
	LULC k	Xk,1	Xk,2	Xk,3	…	**Xk, k**	Xk+	XK, K/Xk+
Column total x+j		X+1	X+2	X+3	…	X+K	N	
Producers' accuracy (%)		X1,1/X1+	X2,2/X2+	X3,3/X3+	.	XK, K/Xk+		

Where:

- k - classes in the remote sensing–derived thematic map
- N -ground reference test samples that are used to assess its accuracy

- Cell entry, xij, is proportion of area mapped as class i & labelled class j in z reference data.
- The row marginal, xi+, is the sum of all xij values in rows i and represents the proportion of area classified as class i.
- The column marginal, x+j, is the sum of all xij values in column j and represents the proportion of area that is truly class j.
- The diagonal, xii, summarizes correctly classified pixels.
- All off diagonal cells represent misclassified pixels.

3.4.4. Change Detection and Analysis

To determine the extent of the occurred LULC change within the study area, a change detection procedure was utilized. Provided with the ArcGIS 10.8 software, the object-based change detection technique was chosen as the most suitable technique for this specific study. The only difference of these technique from the pixel-based change detection technique is that the image is not classified by each specific pixel but over the segmentation of all the combined pixels as objects and afterward running the classification on those objects (Lillesand et al., 2015; Ban, 2016); which are the two vital steps for object-based change detection technique and as a result incorporates spatial neighborhood properties (Blaschke, 2010; Simbangala et al., 2015).

The object-based technique was frequently adopted in a number of studies with very effective outcomes ranging from a decrease in variances found within each class, a more effective classification process particularly with multispectral imagery and the related algorithms were simple and ease to utilize (Duro, 2012). Equally, studies that utilized pixel-based techniques and compared with the results generated by the object-based technique have found that the object-based technique outperforms the previous methods, precisely with regard to the overall accuracy of the classification in a variety of environmental and urban settings (Duro, 2012).

Henceforth, following the object-based technique, the post classification comparison (PCC) method that uses a 'pixel-by-pixel' comparison method so as to detect areas of LULC transformations (Kercival, 2015)were used in this study. The main reason behind is that, PCC enables the process of comparative analysis of the satellite imagery obtained in a time series to occur after the previous independent classification (Dissanayake, 2020). In a study conducted by (Kercival, 2015).the method of PCC was applied because it was identified as the

only change detection method that allowed for classes to be calculated based on how each pixel had been changed from each of the relevant classes.

Additionally, the cross-tabulation were done by selecting pixel by pixel in pairs of two different years as modelled in table 4 below. The LULC change including urban sprawl, agricultural land at urban fringe, and LST were analyzed in detail.

Table 4: General LULC transition matrix to compare two maps among observation times

		Land Class Year time 2 (T2)					Row total xi+
		LULC 1	**LULC 2**	**LULC 3**	**……**	**LULC k**	
Land Class Year time 1 (T1)	**LULC 1**	X1,1	X1,2	X1,3	…..	X1, k	X1+
	LULC 2	X2,1	X2,2	X2,3	…..	X2, k	X2+
	LULC 3	X3,1	X3,2	X3,3	……	X3, k	X3+
	.	.	.	.	.	.	.
	LULC k	Xk,1	Xk,2	Xk,3	…….	Xk, k	Xk+
Column total xj+		X+1	X+2	X+3	……	X+K	**Area Tot**

Where:

- *X= Area of land use land cover in hectares in each cell*
- *xi+ = sum of row*
- *xj+ = sum of column*

3.4.5. LST Retrieval from Thermal Band.

Accordingly, LST was retrieved using digital numbers (DN) of the thermal band of Landsat 5 TM (band 6), Landsat 7 ETM + (band 6_1) and Landsat 8 OLI (band 10) that acquired by 120 m, 60 m and 100 m resolution respectively, but all of those resampled to 30 m resolution. Landsat 5 TM and Landsat 7 ETM + have one thermal band (band 6) while Landsat 8 OLI/TIRS has two thermal bands (bands 10 and 11). Specifically, the Mono Window Algorithm (MWA) methodology to retrieve LST, TM band 6, ETM + band 6_1 (high gain) and TIRS band 10 was used for this study. The LST retrieval equations explained bellow was used for the retrieval.

Conversion of the DN to Spectral Radiance (Lλ)

Digital data formatted for distribution to the user community present pixel values as digital numbers (DNs), expressed as integer values to facilitate computation and transmission and to scale brightness's for convenient display (Campbell, 2011). As stated by Campbell, (2011) and Bonafoni and Sekertekin, (2020) DNs can be converted to radiances using data derived from

the instrument calibration provided by the instrument's manufacturer. Accordingly for a given sensor, spectral channel, and DN, the corresponding radiance value (L) can be calculated as(Qin, Karnieli and Berliner, 2001; USGS, 2019b, 2019a; Ouma et al., 2021):

$$L\lambda = \left(\frac{L_{MAX} - L_{MIN}}{QCAL_{MAX} - QCAL_{MIN}} \right) * (QCAL - QCAL_{MIN}) + L_{MIN}$$

Where *L*MAX = maximum spectral radiances (15.600 for TM and 17.04 for ETM +),

*L*MIN = minimum spectral radiances (1.238 for TM and 0 for ETM +),

QCALMAX = maximum Digital Number (DN) value (255),

QCALMIN = minimum Digital Number (DN) value (1),

QCAL = Digital Number of bands 6.

For Landsat 8 OLI/TIRS thermal band, top of atmospheric radiance ($L\lambda$) will be calculated by the method provided by (USGS, 2019b):

$$L\lambda = M_L * QCAL + A_L$$

where *ML* = band-specific multiplicative rescaling factor (0.0003342);

QCAL=digital numbers of band 10, *AL*=band-specific additive rescaling factor (0.1).

All of these variables can be retrieved from the metadata file of Landsat 8 data.

Top of Atmosphere Brightness Temperature (ToB)

After radiance conversion, TOB temperature, which is the effective temperature viewed by the satellite under assumption of unity emissivity. Conversion of Spectral Radiance (Lλ) to at Satellite Brightness Temperature the equation(Qin *et al.*, 2001; Li, Zhang and Kainz, 2012):

$$T_B = \frac{K_2}{\ln\left(\frac{K_1}{L\lambda} + 1 \right)}$$

where: T_B = Top of atmosphere brightness temperature in Kelvin (K):

$L\lambda$ = TOA spectral radiance (Watts/ (m^2 * srad * μm))

K_1 = Band-specific thermal conversion constant from the metadata (K_1_Constant_Band_x, where x is the thermal band number)

K_2 = Band-specific thermal conversion constant from the metadata (K_2_Constant_Band_x, where x is the thermal band number)

K_1 and K_2 are calibrated constant depending on the sensor of TM, ETM$^+$ and OLI. The values of $K1$ and $K2$ were 607.76 and 1260.56 for Landsat 5 TM, 666.09 and 1282.71 for Landsat 7 ETM $^+$, 774.89 and 1321.08 for Landsat 8 OLI, respectively(USGS, 2019a, 2019b).

Calculation of Land Surface Temperature (LST)

Obtained brightness-temperature must be corrected for spectral emissivity (ε) to determine LST. The algorithm used by Artis and Carnahan, (1982) has followed to calculate emissivity corrected LST; emissivity correction depends upon the nature of the land cover and it is done by using Normalized Difference Vegetation Index (NDVI) values for each pixel. The equation to compute the emissivity corrected land LST is:

$$S_T = \frac{T_B}{1 + \left(\frac{\lambda * T_B}{r}\right) * \ln \varepsilon} - 273.15$$

where ST = land surface temperature in (°C), TB = at satellite brightness temperature (K),

λ = wavelength of emitted radiance in meters (11.5 μm), $\rho = 1.438 \times 10^{-2}$ mK,

ε = emissivity (ranges from 0.97 to 0.99). Emissivity can be expressed with equation:

$$\varepsilon = 0.004Pv + 0.986,$$

where PV = proportion of vegetation and it is calculated by equation:

$$P_V = \left(\frac{NDVI - NDVI_{MIN}}{NDVI_{MAX} + NDVI_{MIN}}\right)^2$$

Emissivity and Proportion of vegetation are calculated by following (Sobrino *et al.*, 2004).

3.4.6. Calculation of NDVI and NDBI

For the purpose of this study two remote sensing-based indices will be combined: NDVI and NDBI. This blend takes advantage of the unique spectral responses of built-up areas and other land cover types(Viana et al., 2019; Guha et al., 2020); used to characterize land cover class associated with LST. Builtup areas are effectively mapped through arithmetic manipulation of the indices derived from TM, ETM$^+$ and OLI sensor data. The Vegetation indexes NDVI calculated as:

$$NDVI = \frac{B_{NIR} - B_{RED}}{B_{NIR} + B_{RED}}$$

where NIR = the near infrared band of the image (TM band 4, ETM $^+$ band 4, OLI band 5),

RED = red band of the image (TM band 3, ETM $^+$ band 3, OLI band 4).

NDBI is sensitive to built-up area and used as an indicator of built-up extent and used widely(Rasul and Ibrahim, 2017). NDBI values vary between −1 and +1 and calculated as (Chen et al. 2006):

$$NDBI = \frac{B_{SWIR} - B_{NIR}}{B_{SWIR} + B_{NIR}}$$

where SWIR1= shortwave infrared band of image1 (TM band 5, ETM $^{+}$ band 5, OLI band 6),

NIR = near infrared band of the image (TM band 4, ETM $^{+}$ band 4, OLI band 5).

Both selected indices (NDVI and NDBI) are presented in an equivalent scale, with values ranging from -1 to 1, simplifying comparisons. Since data from three different sensors were used in this study (Landsat 5, Landsat 7 and Landsat 8) different bands are retrieved to derive the corresponding indices(Viana et al., 2019).To investigate the relationship between LST and different land cover indices, randomly selected points methods will be applied following and using the Pearson's correlation coefficient.

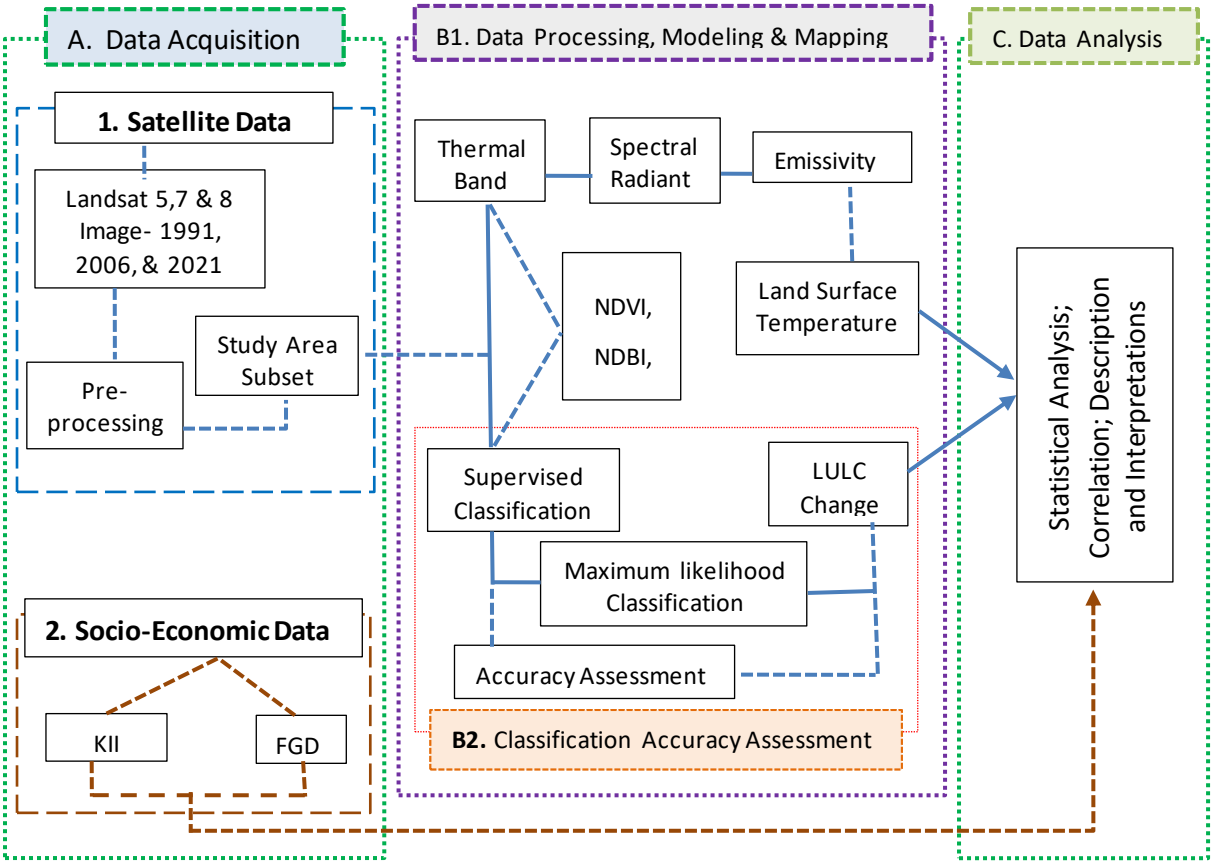

Figure 5: Methodological Flow Chart of the Study

CHAPTER FOUR

4. RESULTS AND DISCUSSION

4.1. Land Use Land Cover (LULC) Classification

The final classified map was generated by showing different land cover types in Woliso Town and adjacent rural district areas for the years 1991, 2006 and 2021. Accordingly, the land-use land-cover classification result of the1991 showed that the dominant LULC classes were agricultural land and forest land. These classes accounted for 9492.76 hectares which is 68.8% and 2514.25 hectares 18.2% of the overall area coverage of 13793.6 hectares respectively. The wet & grassland accounted 807.1 hectares 5.8%. However, the Built-up area were 691.2 hectares 18.2% whereas dry bare land were 288.5 hectares 2% of the total area coverage.

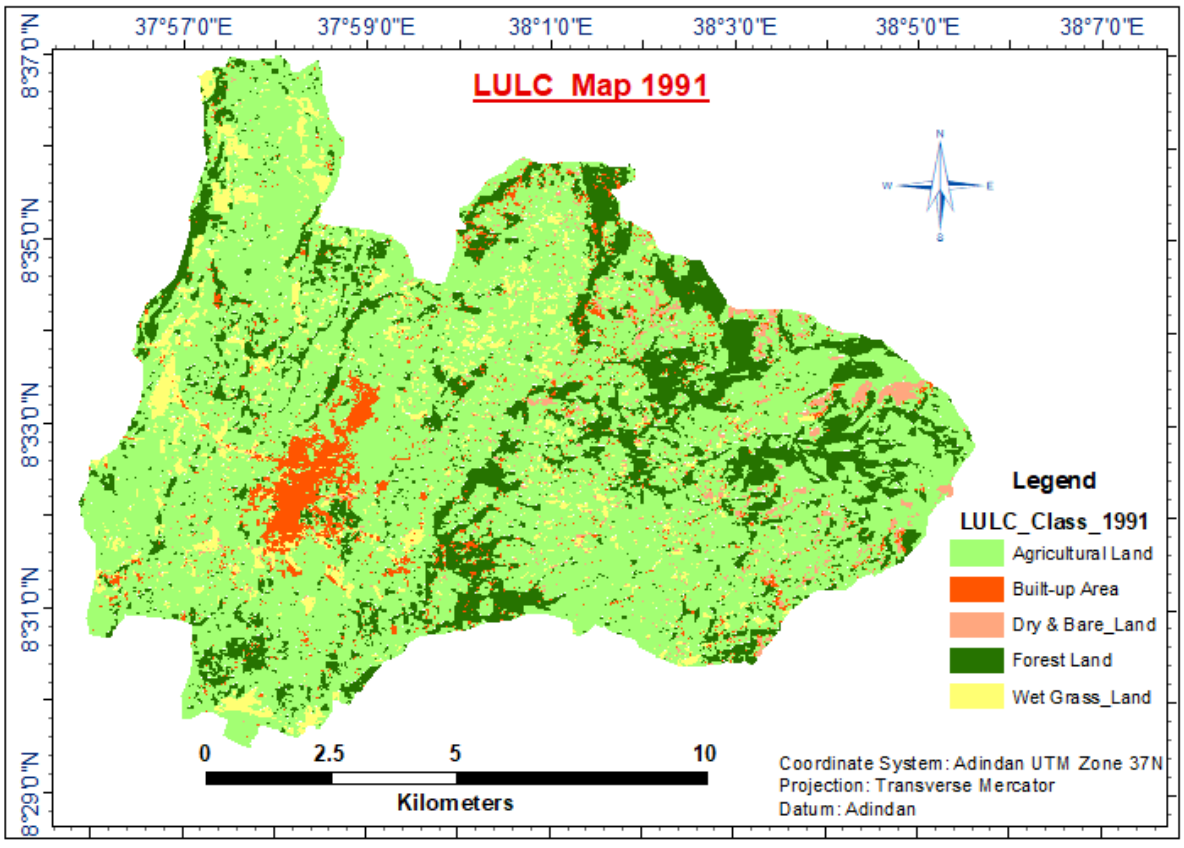

Figure 6: LULC classification Map of Woliso Town Area 1991

Table 5: LULC_ Area Coverage in hectare 1991 Year and percentage

FID	LULC Class_1991	Area_1991 (he)	Percentage
1	Agricultural Land	9492.76	68.82
2	Built-up Area	690.81	5.01
3	Dry Bare Land	288.53	2.09
4	Forest Land	2514.26	18.23
5	Wet Grassland	807.13	5.85
Total		13793.50	100.00

In the 2006 LULC classification outcome water body also covered the smallest and insignificant area of all other classes. The classification revealed that the dominant LULC categories were agricultural land 9450.7 hectares (68.5%); forest land 2014.6 hectares (14.6%), followed by built-up area 1056.74 hectares (7.6%) of the total area coverage. The other LULC classes were dry and bare land which accounted 765.19 hectares (5.55%) whereas that of wet and grassland area was recorded to be only 506.19 hectares (3.67%) of the total area.

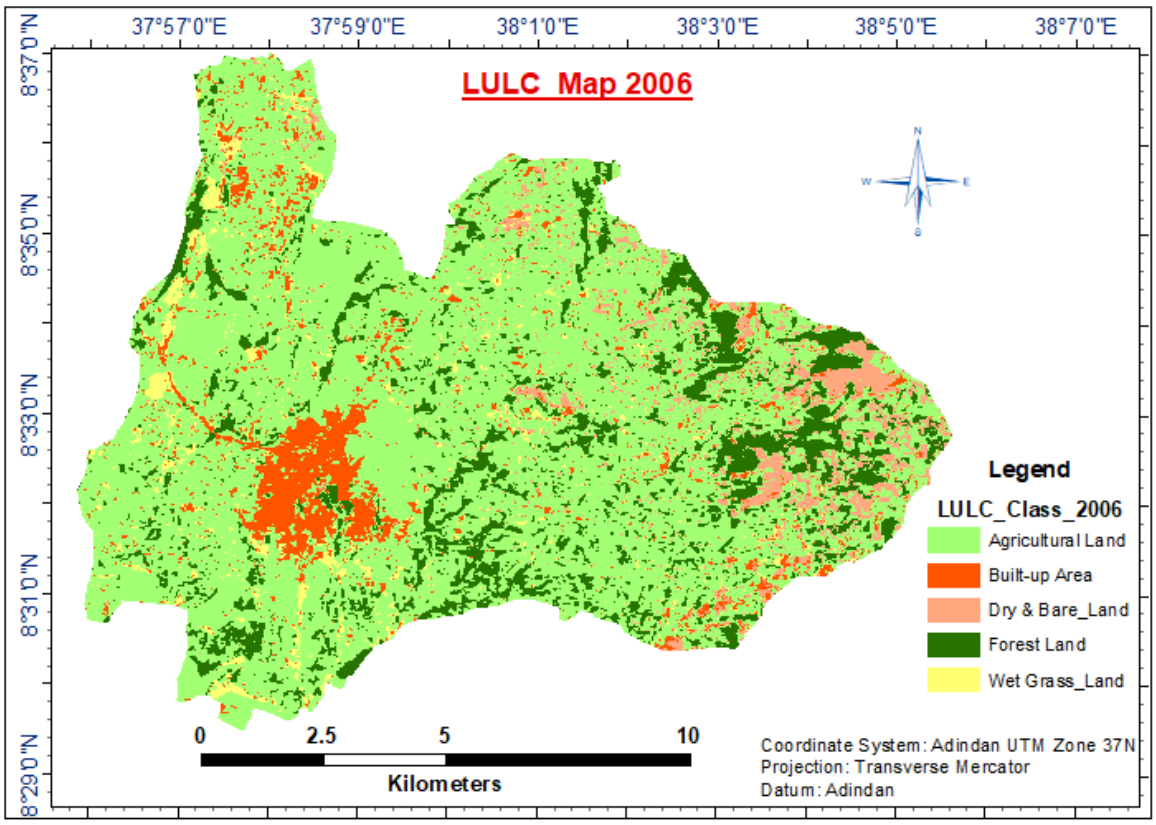

Figure 7: LULC classification Map of Woliso Town Area 2006

Table 6: LULC_ Area Coverage in hectare 2006Year and percentage

LULC_2006			
FID	**Class_2006**	**Area_2006 (he)**	**Percentage**
1	Agricultural Land	9450.73	68.52
2	Built-up Area	1056.74	7.66
3	Dry Bare Land	765.19	5.55
4	Forest Land	2014.66	14.61
5	Wet Grassland	506.19	3.67
Total		13793.50	100.00

Finally, the 2021 Land-use land-cover classification result implied that the agricultural land, wet and grassland as well as forest land became diminished from the 1991 LULC classification results. In contrary to these the built-up area including dry and bare land has revealed as increment. For LULC classification detailed statistical data for each of these classes and LULC map of the study period shown in Figure 8 and Table 7 below.

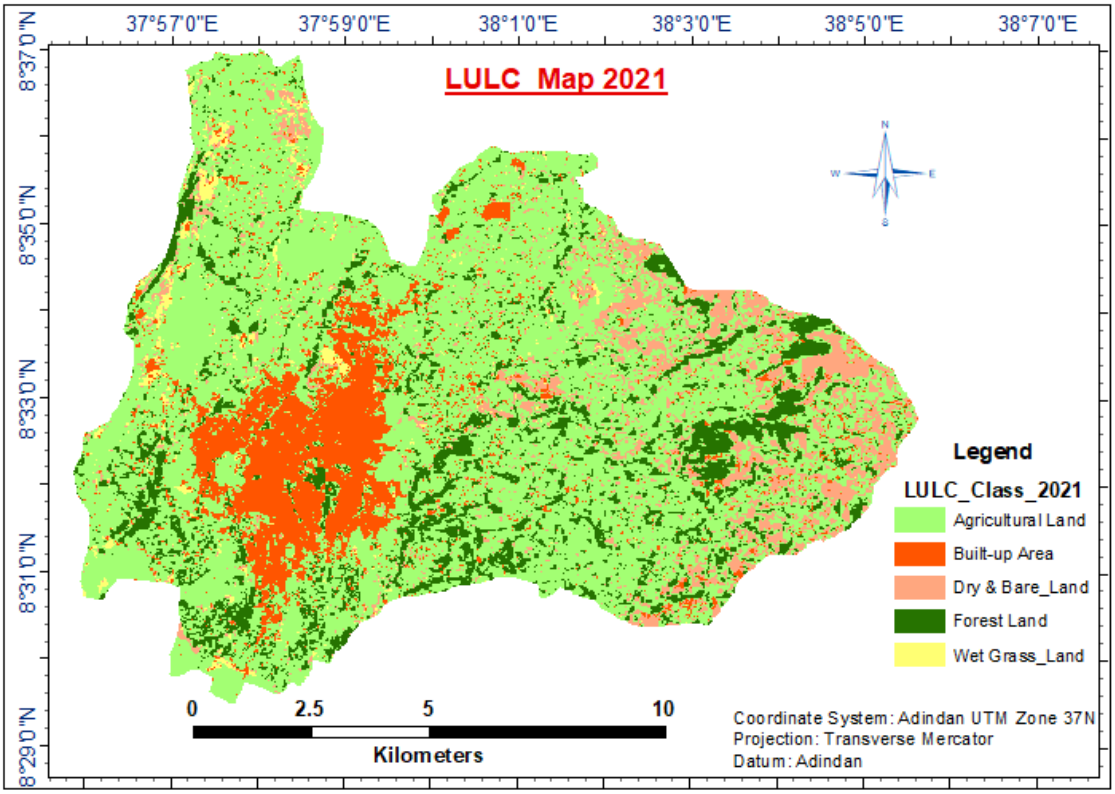

Figure 8: LULC classification Map of Woliso Town Area 2021

Thus, in the 2021 LULC classification agricultural land accounted 8582.78 hectares (62.22%), forest land 1825.06 hectares (13.23%) as well as wet grass land 277.06 hectares (2.01%) of the total coverage consequently. The built-up area was recorded to be 1795.82 hectares (13.02 %) where as dry and bare land was 1312.78 hectares (9.52%) both showing drastic increments.

Table 7: LULC_ Area Coverage in hectare 2021Year and percentage

LULC_2021			
FID	**Class_2021**	**Area_2021 (he)**	**Percentage**
1	Agricultural Land	8582.78	62.22
2	Built-up Area	1795.82	13.02
3	Dry Bare Land	1312.78	9.52
4	Forest Land	1825.06	13.23
5	Wet Grassland	277.06	2.01
Total		13793.50	100.00

The tabulated chart as Figure 9 showed the area in hectares for different land cover classes for the 1991, 2006 and 2021 years below.

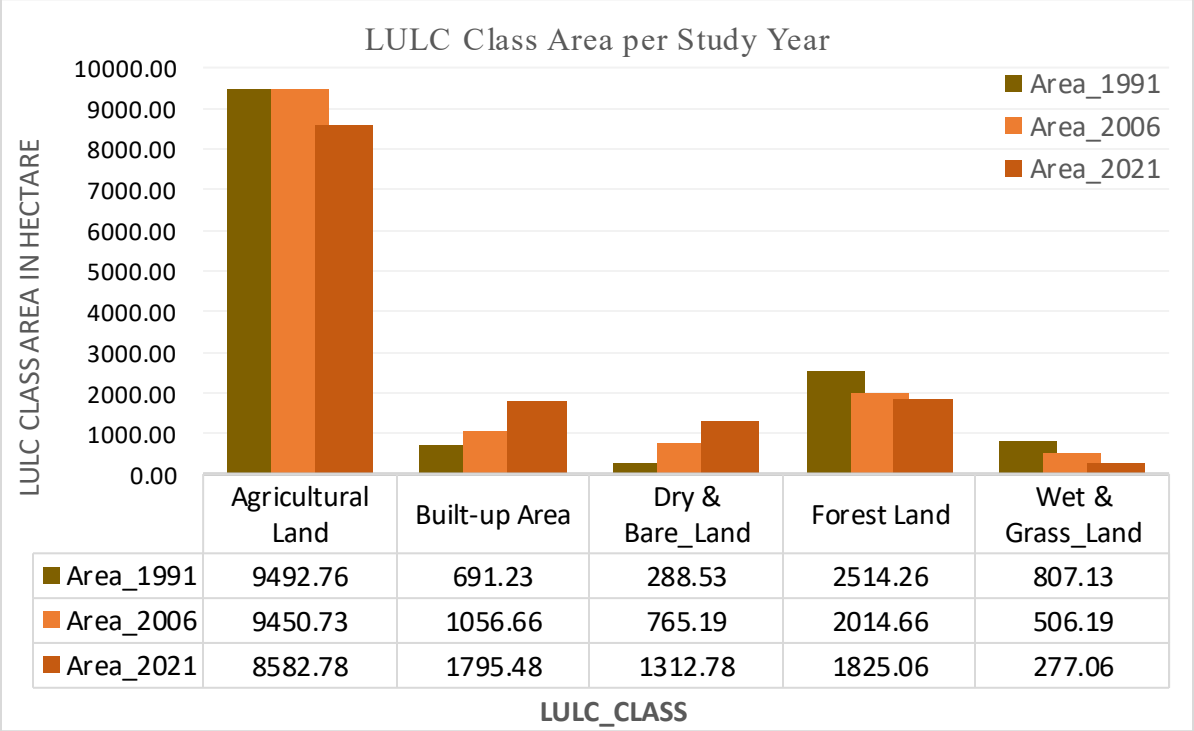

Figure 9: Tabulated chart of LULC analysis in Woliso Area during 1991, 2006 and 2021

4.2. Land Use Land Cover Changes

LULC changes were computed for the years 1991, 2006 and 2021, focusing on Agricultural land, Built-up area, Forest Land, Wet & Grass land and Dry and bare land. The cumulative change calculated in agricultural land was approximately -909.98 (Area 1991 - Area 2021), which was 9492.76 hectares (1991) and 8582.78 hectares (2021) with an inverse accumulative change of 9.5 % between 1991 and 2021-year periods. The built-up area was calculated to be 691.23 hectares in 1991 and 1795.48 hectares in 2021, with an increase change of 1104.25 hectares between 1991 and 2021 (Table 8).

The forest area was calculated to be approximately 2514.26 hectares in 1991, 2014.66 hectares (2006) and 1825.06 hectares (2021), with periodic decrement from 1991–2021-year periods. Similarly wet and grassland showed periodic decline as recorded to be 807.13 hectares (1991), 506.19 hectares (2006) and 277.06 hectares (2021). In contrary to both forest land and grass-land the dry and bare land showed periodic increment like the built-up area. Statistically it was recorded 288.53 hectares (1991), 765.19 hectares (2006) and 1312.78 hectares (2021).

The chord wheel illustrates the results of the various land use categories for different years in proportion to others with respect to different LULC class (Figure 10); Whereas Table 8 illus-trates LULC area coverage in year and percentage coverage difference per study period as shown below.

Table 8: LULC_ Area Coverage in Year and percentage Coverage difference

LULC_1991, 2006 and 2021									
ID	**LULC Class**	**Area 1991**	**%**	**Area 2006**	**%**	**Area 2021**	**%**	**Change 2006-1991**	**Change 2021-1991**
1	Agricultural Land	9492.76	68.82	9450.73	68.52	8582.78	62.22	-42.03	-909.98
2	Built-up Area	690.81	5.01	1056.74	7.66	1795.82	13.02	365.92	1105.01
3	Dry Bare Land	288.53	2.09	765.19	5.55	1312.78	9.52	476.66	1024.25
4	Forest Land	2514.26	18.23	2014.66	14.61	1825.06	13.23	-499.60	-689.20
5	Wet Grassland	807.13	5.85	506.19	3.67	277.06	2.01	-300.95	-530.08

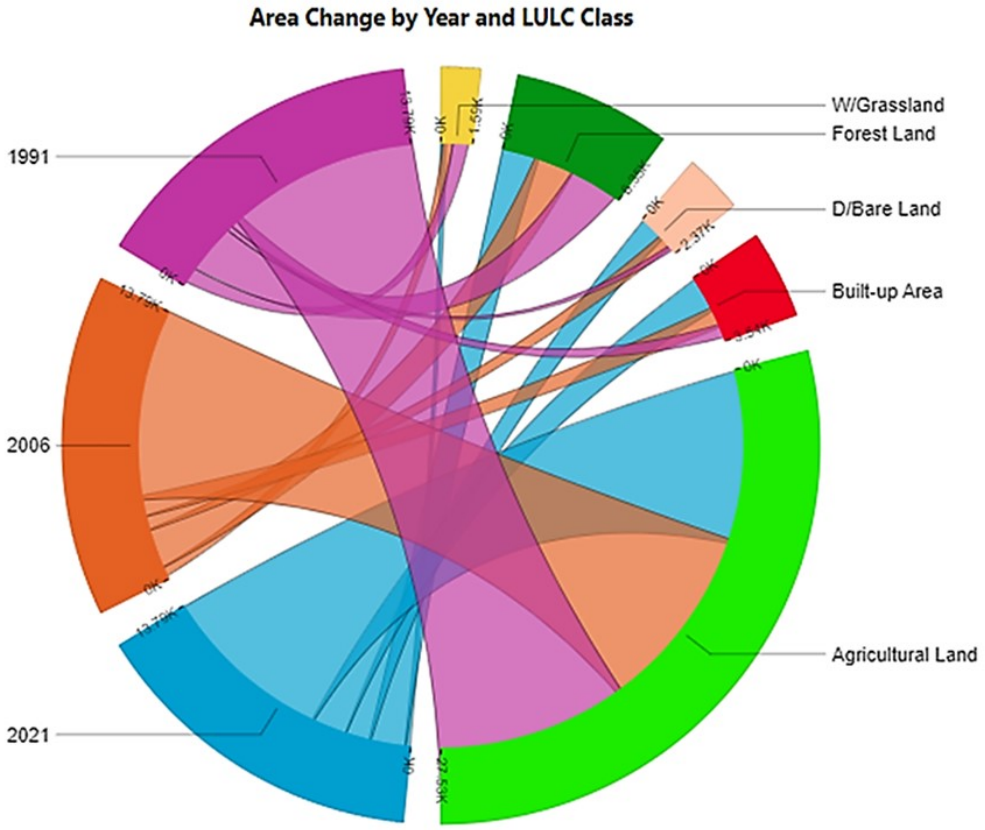

Figure 10: The Chord Diagram clarifies the portion of LULC Changes concerning the time series 1991, 2006 and 2021 with respect to LULC classes.

The results revealed by (Yesserie, 2009; Getu, 2014; Halefom et al., 2018) showed that conversions of land from agriculture to urban land due to urban expansion and sprawl led to higher loss of agricultural land which negatively affected the pattern of land use (Kebebew, Worku and Babu, 2019) represent the most prominent land cover change with a continuous decreasing. Similarly, as shown by transition matrix (table 9, 10, 11 and Figure 12) this study implied that in the year 1991 to 2006 about 585.9 hectares of agricultural land was converted to the built-up area where as from 1991 to 2021 about 1186.47 hectares was converted to built-up area. Equally, about 160.99 hectares of wet and grassland in the year 1991 to 2021 were converted to the built-up area. Likewise in line with the work of (Boori et al., 2015; Samanta and Pal, 2016; Gashu and Egziabher, 2018) due to rapid prevalence of urban sprawl and other settlement area primary forests have been affected. In the study area 100.19 hectares of forest lands between the year 1991 to 2021 were converted to the built-up area in 30-year intervals. In contrary to this and in contradiction of results reveled by (Rahman, 2016a) only minimal

quantity of dry and bare land was converted to the built-up area showing rapid urbanization was consuming valuable land spaces.

As seen from table 8 and figure 10 the agricultural land appeared as being maintained 68.82% (1991), 68.52% (2006) and seemed minimal change 62.22% (2021) but it was at the expense of other LULC classes. As shown by transition matrix bellow about 453.63 hectares (1991-2021) of wet and grassland and about 1262.79 hectares (1991-2021) of forest lands were converted to the agricultural land which is in line with (Yesuph and Dagnew, 2019). Additionally, during the 1991 regime change in Ethiopia most of the rural settlement re-scattered to their original settlement and some other factors some built-up area about 268.04 hectares (1991-2021) was converted to agricultural land. Furthermore about 113.6 hectares of dry and bare land was converted to agricultural land. And hence the sum of all these conversions to agricultural land pretended it as being sustained.

The forest area was calculated with estimate showing periodic minimal decrement from year 1991 to 2021 as expressed above. But the reality was that considerable quantity of agricultural land about 585.8 hectares (1991 to 2006), 754.2 hectares (1991 to 2021) was converted to eucalyptus tree plantation and **khat** (local name chaat) production showing the spectral reflectance band as forest land which implies the prevalence of extreme distraction on natural forests.

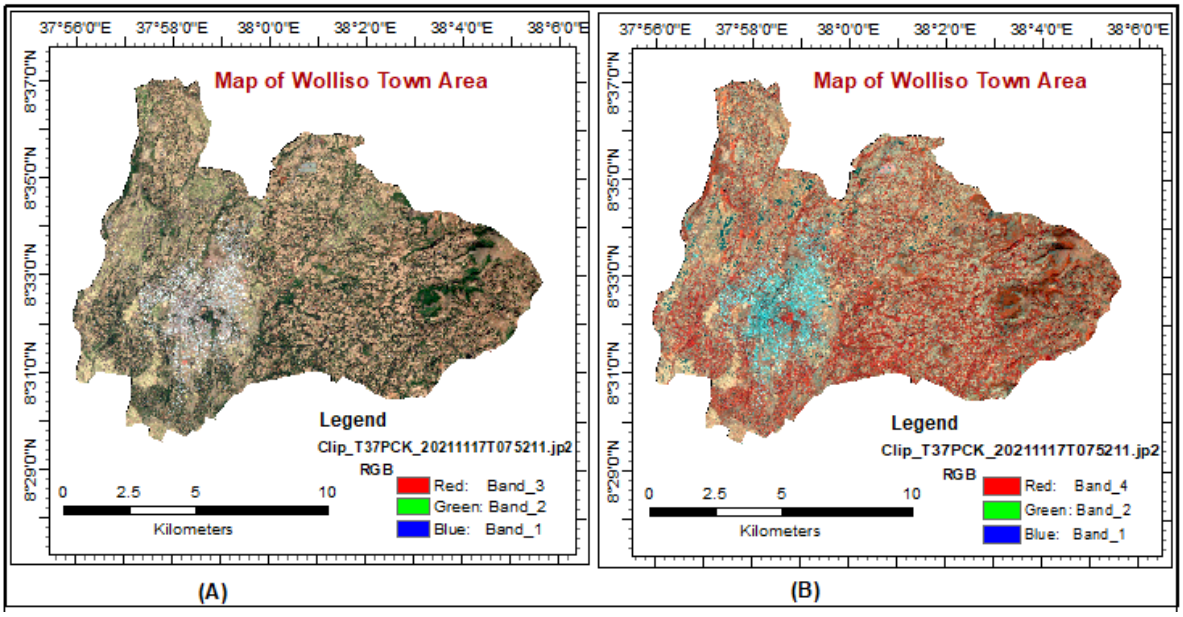

Figure 11: Maps Sentinel-2 satellite image (10-m SR) of 2021 (**A**) True Color (**B**) False color

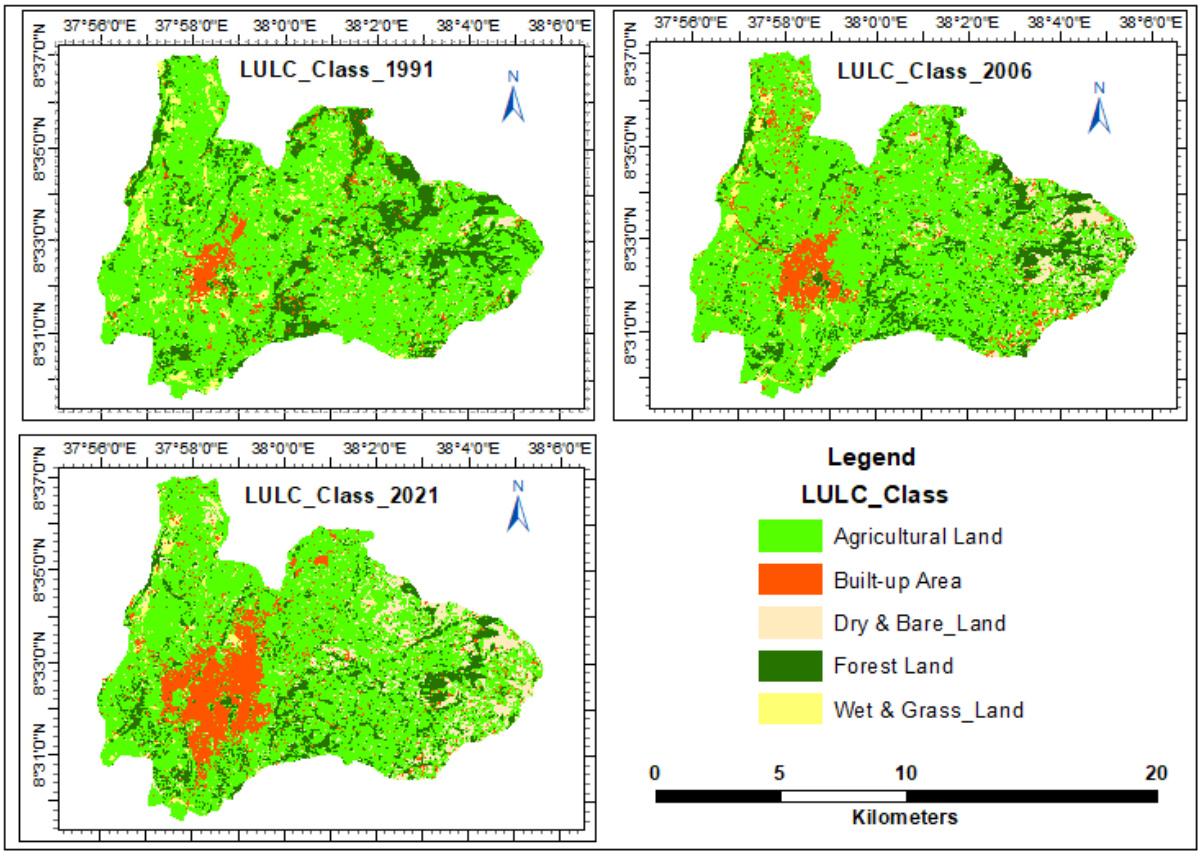

Figure 12: LULC Change maps for 1991-, 2006- and 2021-year periods

The land use land cover change matrix illustrated in Table 9, Table 10 and Table 11 for the periods 1991 – 2006, 2006 – 2021 and 1991 – 2021 respectively bellow displays the distribution of main transitions in the 5 (five) LULC classification categories used in this study which has revealed that there were major changes and transition among the LULC classes. The water body LULLC class was excluded due to insignificant quantity (0.0001 hectare) showing more decrement on successive study period in the study area. The portion of LULC Area Changes regarding the LULC Class from 1991 to the LULC Class 2021 for the entire study period is shown as tabulated chart on Figure 12 bellow.

Table 9: Land use and land cover change transition matrix between 1991 and 2006

Land Class Name		Land Class of 2006					Grand Total
		Agriculture	Built-up area	Bare Land	Forest Land	Grassland	
Land Class of 1991	Agriculture	**7320.16**	585.90	570.40	696.59	309.69	**9482.75**
	Built-up Area	356.47	**263.50**	21.06	35.97	13.82	**690.83**
	Bare Land	136.72	36.40	**101.58**	3.85	9.77	**288.31**
	Forest Land	1161.19	33.84	44.50	**1257.17**	14.82	**2511.53**
	Grass Land	466.60	136.11	26.96	19.17	**157.61**	**806.43**
	Grand Total	**9441.14**	**1055.74**	**764.50**	**2012.75**	**505.72**	**13779.94**

Note: The bold highlighted diagonal numbers show the unchanged LULC proportions from 1991- 2006

Table 10: Land use and land cover change transition matrix between 2006 and 2021

Land Class Name		Land Class of 2021					Grand Total
		Agriculture	Built-up area	Bare Land	Forest Land	Grass-land	
Land Class of 2006	Agriculture	**6843.27**	1017.74	706.70	734.93	139.91	9442.55
	Built-up Area	342.79	**561.01**	95.86	18.02	37.94	1055.63
	Bare Land	301.43	61.52	**368.70**	20.33	12.05	764.02
	Forest Land	831.86	76.79	62.74	**1036.21**	4.63	2012.23
	Grassland	254.96	78.08	76.62	14.04	**82.10**	505.80
	Grand Total	**8574.32**	**1795.13**	**1310.62**	**1823.53**	**276.63**	**13779.94**

Note: The bold highlighted diagonal numbers show the unchanged LULC proportions from 2006 - 2021

Table 11: Land use and land cover change transition matrix between 2006 and 2021

Land Class Name		Land Class of 2021					Grand Total
		Agriculture	Built-up area	Bare Land	Forest Land	Grass Land	
Land Class of 1991	Agriculture	**6475.90**	1186.47	915.02	754.25	152.28	9483.92
	Built-up Area	268.05	**316.31**	46.74	38.57	21.06	690.72
	Bare Land	113.62	30.98	**131.57**	8.58	3.35	288.10
	Forest Land	1262.80	100.19	150.55	**985.82**	11.06	2510.43
	Grassland	453.63	160.99	66.67	36.28	**89.01**	806.58
	Grand Total	**8574.00**	**1794.94**	**1310.54**	**1823.51**	**276.76**	**13779.94**

Note: The bold highlighted diagonal numbers show the unchanged LULC proportions from 1991 - 2021

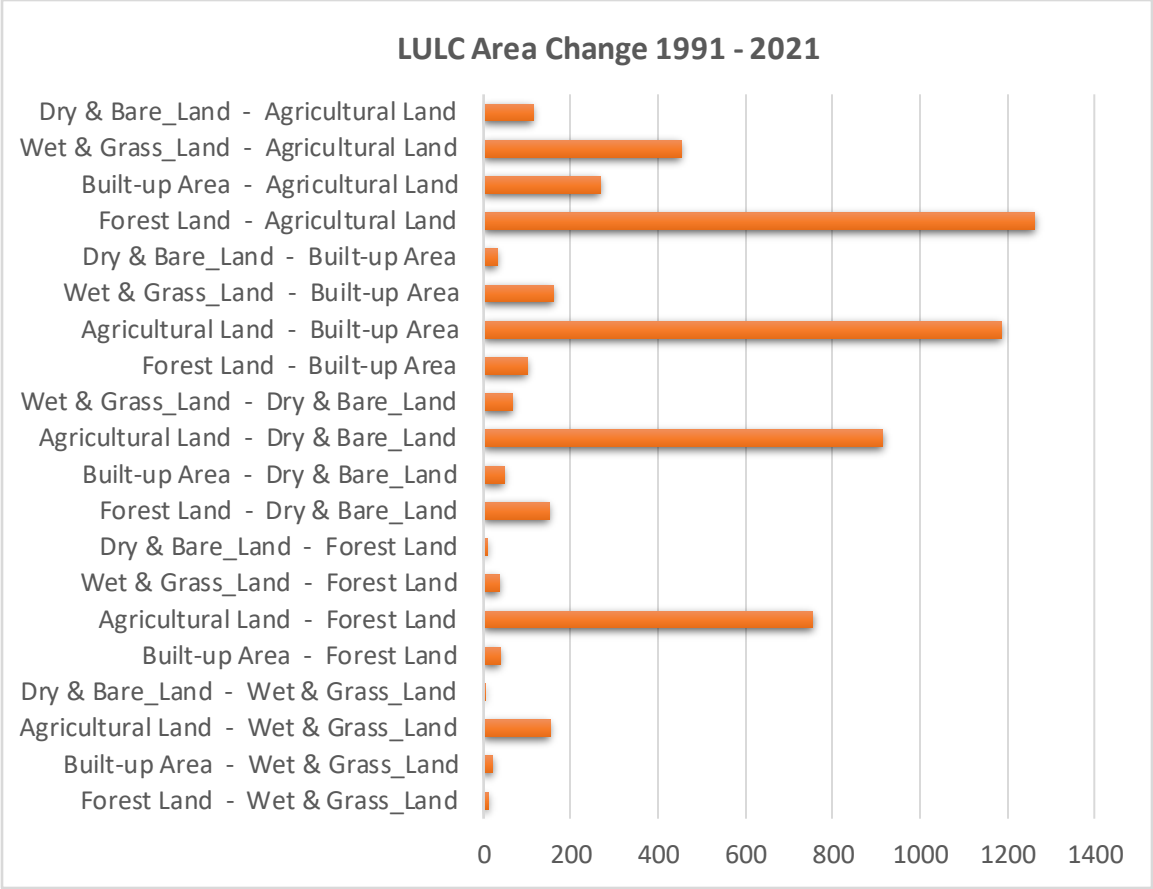

Figure 13: The portion of LULC Area Changes regarding the LULC Class from 1991 to the LULC Class 2021

4.3. LULC Accuracy Assessment

The quality of the thematic map from satellite image is determined by its accuracy and hence the accuracy assessment is a vital step in image classification. Information on the accuracy and precision of the classified maps is essential so as to utilize the generated maps effectively. The results from accuracy assessment of the LULC maps varied among the LULC classes and hence the results of accuracy assessment in this study revealed good outcomes despite some errors which could attributed to spectral confusion among built-up areas and bare lands, among grass lands and agricultural lands and forest lands. Comparing with the minimum 85% accuracy stated by most scholars, the overall accuracy for the year 90.2% (1991), 88.6% (2006), 91.1% (2021) as well as the satellite-derived LULC maps kappa coefficient of 0.874 (1991), 0.863 (2006), and 0.893 (2021) statistics obtained in this study satisfied the minimum accuracy requirements. The results were also acceptable for ensuing and continuous post-classification

comparison of change detection operations. The higher overall accuracy achieved in this study could be attributed to the utilization of more ancillary data during the process of image classification. The LULC classification accuracy assessment confusion matrix for the years1991, 2006 and 2021 is attached as Annex 2 A, B and C part of the appendix.

4.4. LULC Dynamics and Urban Fringes Agriculture

The development agent/ extension worker in the study area justify that most previous valuable farm lands were lost due to rapid urban expansion, productivity of each district reduced though farmers were in the regular orientation and equipped with land plowing tools and yield enhancing inputs. It was evidenced that the rapid growth of the town has been accompanied with rapid urban population growth and urban sprawling, leading to the incorporation of the half part of the four rural districts in the peri-urban of the town. This is in line with (Dadi et al., 2018) this significantly affect the size of the total cultivable land and food crop production.

Concerning the socio-economic influences posed, the impact of urban expansion on the agricultural land as land is the most important economic base for the rural residents is more of pressing. In line with that of (Dejene, 2016) the main problem for the local people as reflected in the FGD, is that most farmers used to earn their livelihoods from their own farm lands and consequently, those who lack the skill or experience to join non-farm businesses may that their livelihoods will deteriorate sooner or later. Outcomes in the earlier study(Gebregziabher, 2014) described that conversion of rural farm lands to urban land use is not only confiscating fringe farmers but also depriving them of their livelihoods, whereas the compensation paid is not enough as the valuation method does not reflect current land market and cost of living in Mekelle city of Ethiopia. Inline most of the purposely selected residents owning agricultural land bounded at urban due to urban boundary expansion explained that their livelihoods were affected due to low compensation of their land during expropriation. Surprisingly, the study revealed that most of the converted lands were for urban residential housing establishments and have not created job opportunity for the affected group. Additionally, they agree that their previous cultural social fabrics disintegrated. To illustrate more the Chord Diagram bellow explicates the portion of LULC area changes concerning the LULC class from 1991 to 2021 (Figure 13).

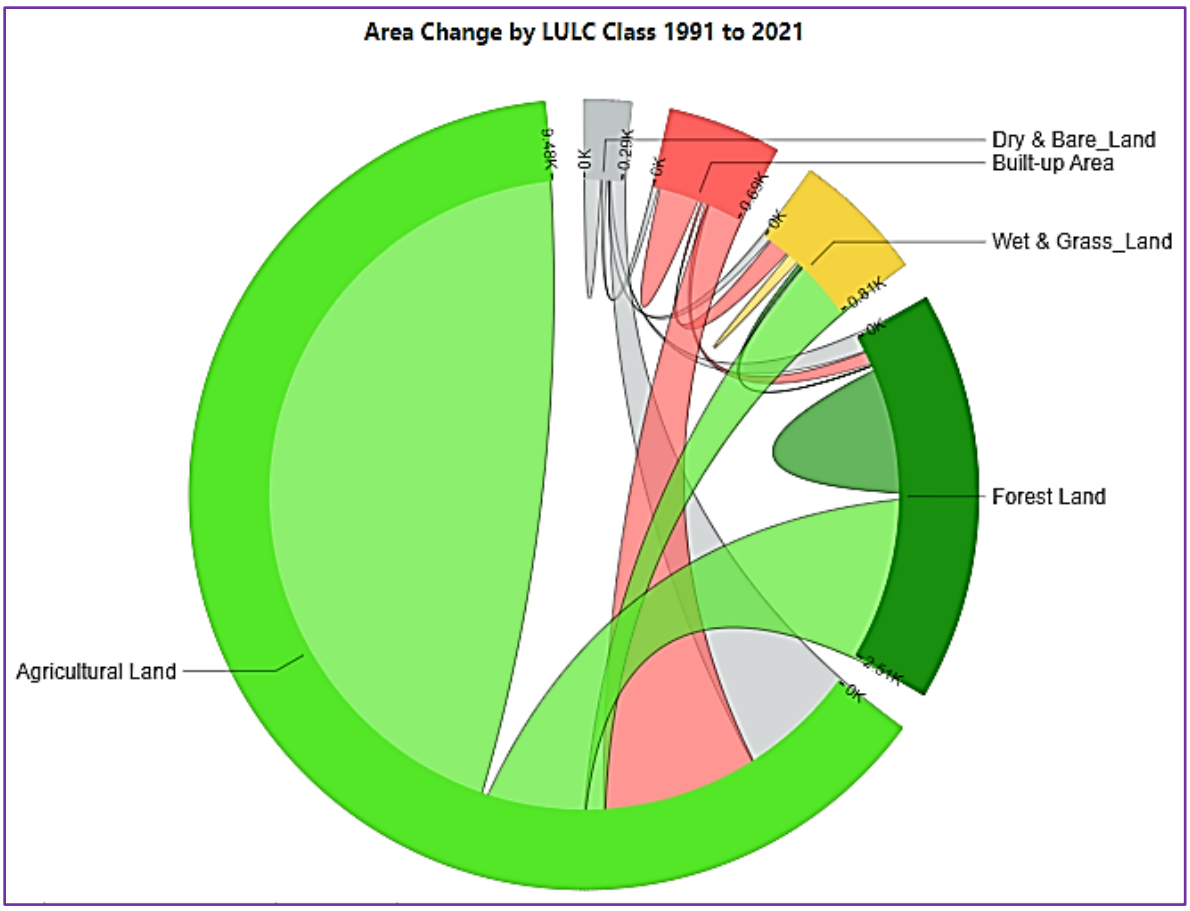

Figure 14: The Chord Diagram explicates the portion of LULC Area Changes regarding the LULC Class from 1991–2021

Generally, it was revealed that Woliso area has experienced severe declines in forest and agricultural land due to urban sprawl over the past three decades. The immense conversion of peri-urban agricultural land and forest land to the built-up areas may have an impact upon urban ecosystem depletion and economic calamity.

4.5. Spatiotemporal Pattern of NDVI

Normalized Difference Vegetation Indices (NDVI) was calculated from Landsat 5TM, 7 ETM^{+} and 8 OLI data whereas only red band and NIR band of Landsat images are used for NDVI analysis in this study. Concerning the results computed, during the years 1991 the NDVI value ranges from −0.0666667 to +0.559055; in 1996 it ranges from −0.0833333 to +0.636364; in 2001 it ranges from −0.044335 to + 0.622047; in 2006 it ranges from −0.173554 to +0.619718; in 2011 it ranges from −0.060869 to +0.602903; in 2016 it ranges from −0.0559192 to

+0.539599 whereas for NDVI values during 2021, it ranges from −0.136883 to +0.527269 correspondingly. Figure 14 bellow shows the normalized difference vegetation index maps of the 1991, 1996, 2001, 2006, 2011, 2016 and 2021 study years successively.

As discussion, the value of the NDVI ranges between -1 and 1. Its values are positive for vegetation including crops, shrubs, grasses, and forests, and are close to zero or negative for non-vegetated areas including rocks, sand, and concrete surfaces (Pettorelli *et al.*, 2005); soil may exhibit nearby zero value, and all water body features have negative values (McFeeters, 1996). Thus, larger NDVI values indicate more vigorous green vegetation cover (Huang *et al.*, 2020). Consequently, focusing on the results reveled in this study the vegetation cover has showed successive and steady decrement from 1991 to 2021 in Woliso area and its surrounding district since the maximum positive value shows stepwise decrement per the study years.

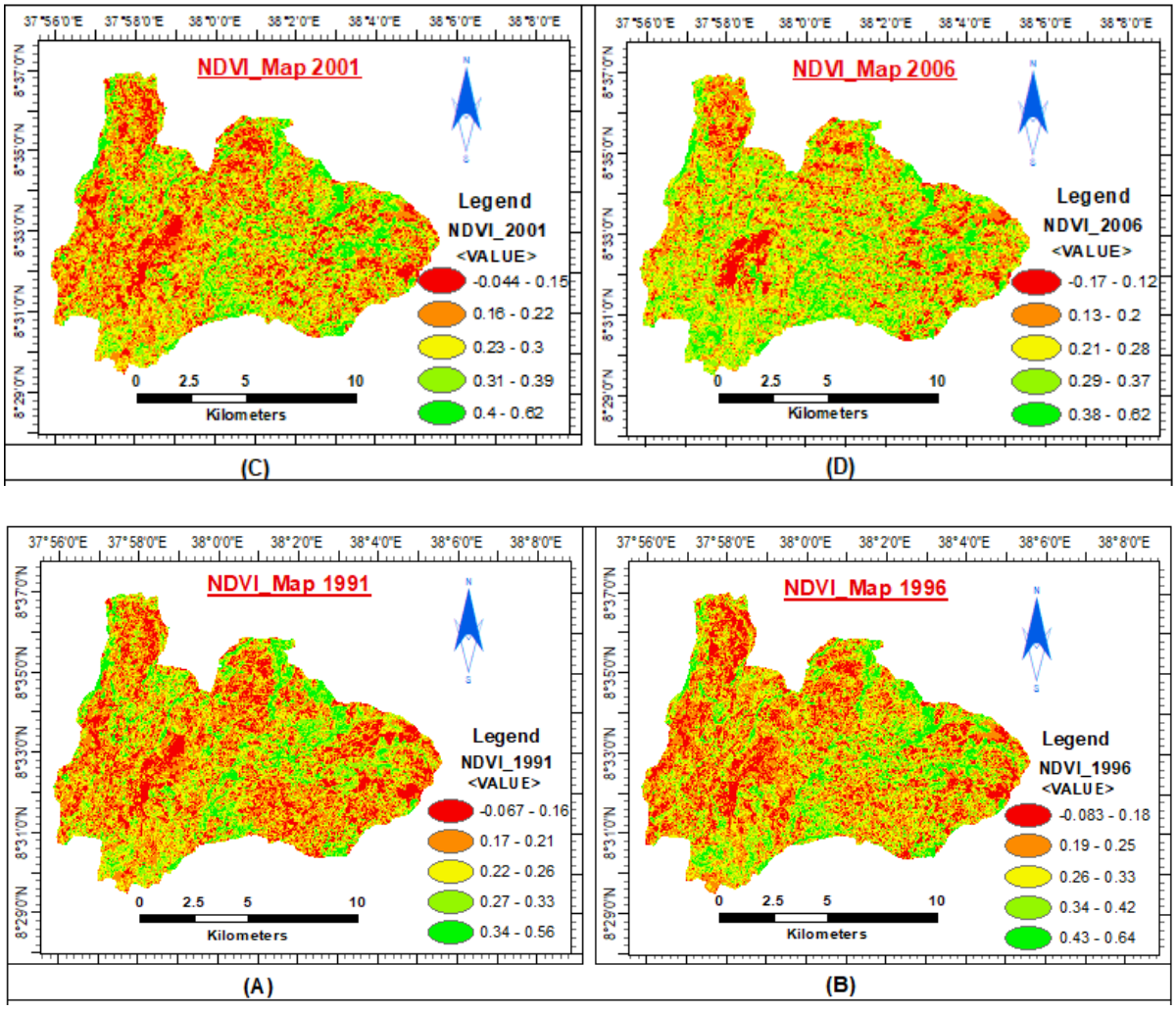

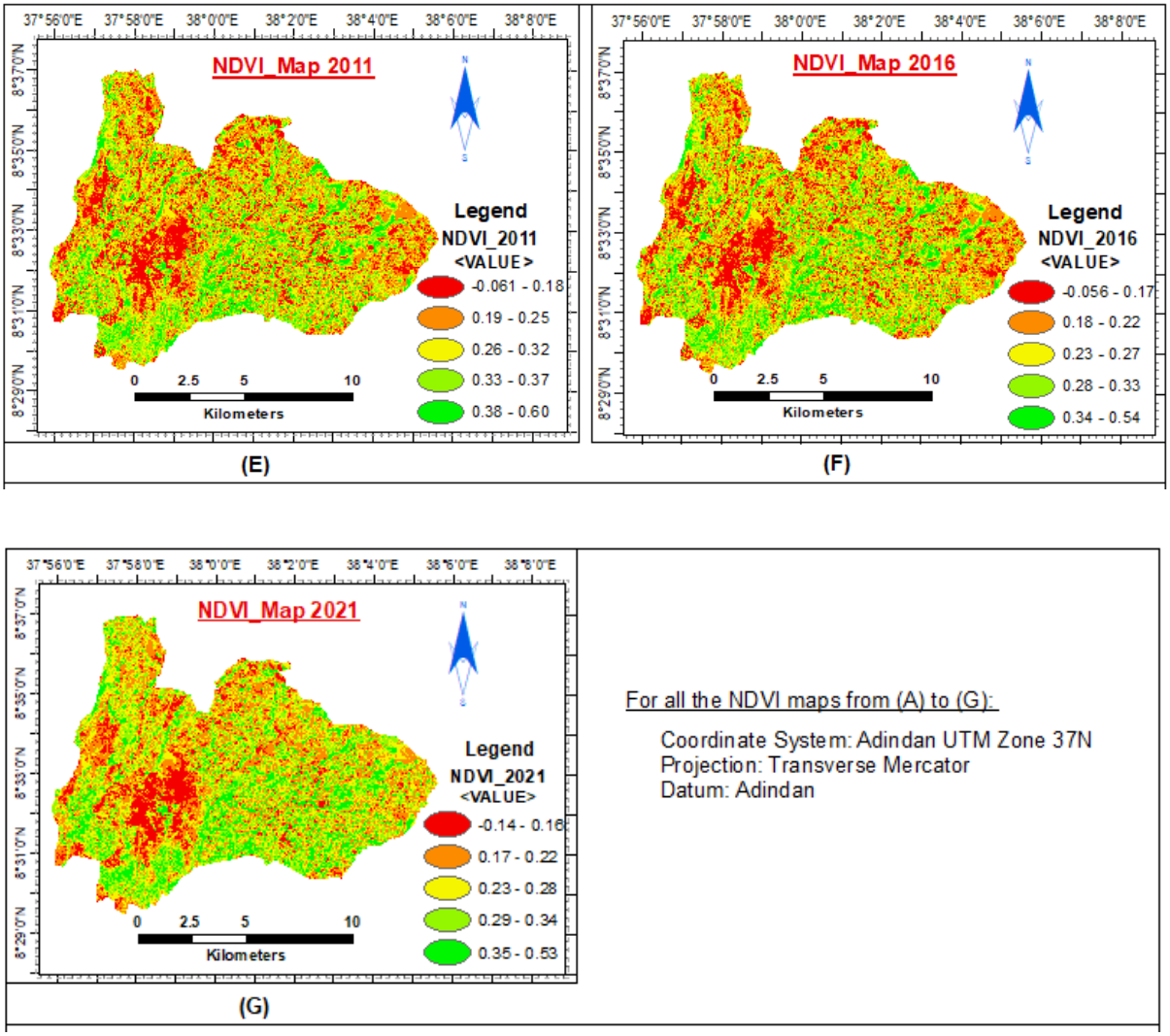

Figure 15: Normalized difference vegetation index maps of 1991, 1996, 2001, 2006, 2011, 2016 and 2021

On the other hand the expression (1- NDVI) indicates that the greater non-vegetative weights to the urban core area rather than to urban peripheral areas, resulting in increased variability of data values in the urban core area (Zhang, Schaaf and Seto, 2013). Therefore, the (1- NDVI) value of urban core areas are close to 1 while that of the non-urban areas rich in vegetation is close to 0. Accordingly, as the results reveled in this study computed with this expression it implied that by way of the gradual decrement in vegetation indicis there is the existence of steady increment in Builtup area and barren land in Woliso area.

4.6. Spatiotemporal Pattern of NDBI

The results of normalized difference built-up index (NDBI) values in the study area per study year were in the range from -0.28 to 0.39 in 1991, from -0.38 to 0.44 during 1996, from -0.29 to 0.46 in 2001, from -0.49 to 0.28 in 2006, from -0.45 to 0.44 in 2011, from -0.37 to 0.25 in 2016 and during 2021 the range was between -0.39 to 0.23 successively.

The value of NDBI ranges between -1 and 1 and most suggests that positive values of NDBI represent urban land areas and negative values of NDBI represent non-urban land areas. Yet, this approach also has some limitations related with recoding the derived NDBI imagery to create a binary image and assuming that positive NDBI value should indicate built-up areas (He et al., 2010); because of this recoding process, the original approach was unable to separate urban areas from barren and bare land. He also noted in his study, the original approach also suffered from commission error, showing some vegetation as built-up area because of the complicated spectral response patterns of vegetation (He et al., 2010).

Having this the NDBI value of the study area showed almost fluctuating results due to different reasons that need further study. From the NDBI map, areas with values greater than zero represent built-up and bare land with NDBI values indicating maroon-colored areas while values below zero or close to zero represent non-built-up area features such as forest land, grassland and agriculture. The NDBI map of the study area for the study period are attached as annex 4 in appendix part of this paper.

4.7. Spatial and temporal distribution of LST pattern

The resulting LST maps for Woliso area are listed below, with the tabulated summary of LST statistics. It was recorded for the years that temperature change was in the range from minimum to maximum in Celsius unit (°C) 11.9 to 30.8 (1991), 13.3 to 31.6 (1996), 11.9 to 30.4 (2001), 14.4 to 34.1 (2006), 12.7 to 36.4 (2011), 14.3 to 31.8 (2016) and 6.05 to 32.4 (2021) consistently. Also, the mean LST for the periods was 22.74°C in 1991, 24.20°C in 1996, 22.43°C in 2001, 25.51°C in 2006, 26.30°C in 2011, 24.44°C in 2016 and 24.81°C in 2021-year period correspondingly. The spatiotemporal variation in LST of 1991, 1996, 2001, 2006, 2011, 2016 and 2021 of study area are shown in Figure 15 consecutively. The Minimum, Maximum and Mean LST in ◦C for each year has shown in Table 12 while the computation of LST (◦C) for each time interval from 1991 to 2021 was illustrated graphically with Figure 16.

Results in the previous study (Imran et al., 2021) reported that Spatial distribution of maximum and mean LST showed increment, during the study period, while the change in minimum LST was not substantial in Dhaka city of Bangladesh. In the case of Woliso area, Spatial distribution of maximum and mean LST experienced fluctuation with incremental trend during total study period of 1991 to 2021. The overall trend of maximum and mean LST showed positive increase of 1.566^{0}C, 2.067^{0}C over the years respectively, but the change in minimum LST was insignificant and declined. From Table 12, the LST is observed to steadily increase over the 30-year period from 1991 to 2021, with a dip in 2001 then increases from 2001-2011, slight dip in 2016 then increases in 2021 with overall trend showing positive increase over the years 2.067^{0}C.

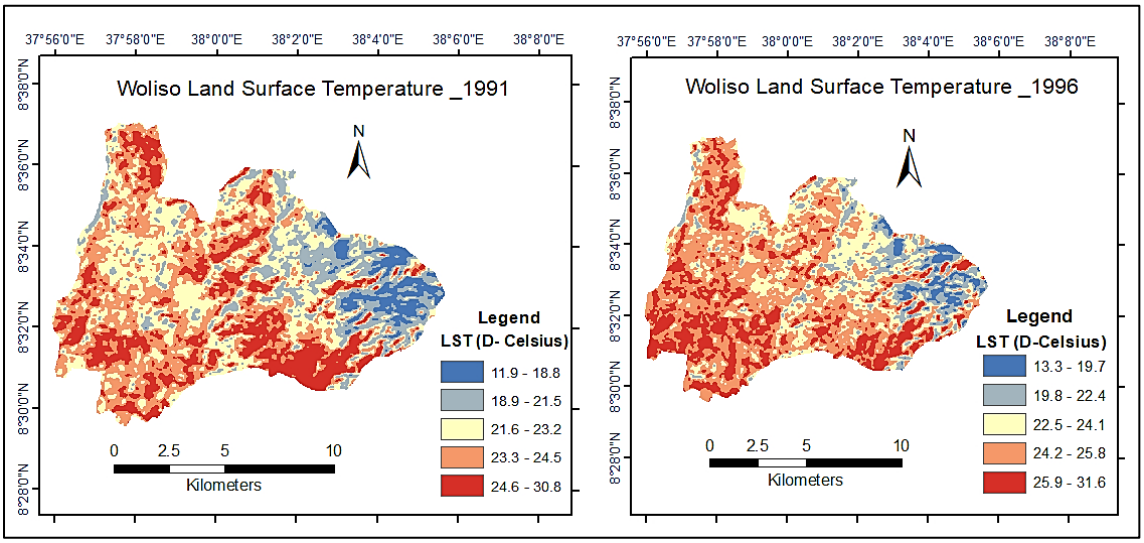

A B

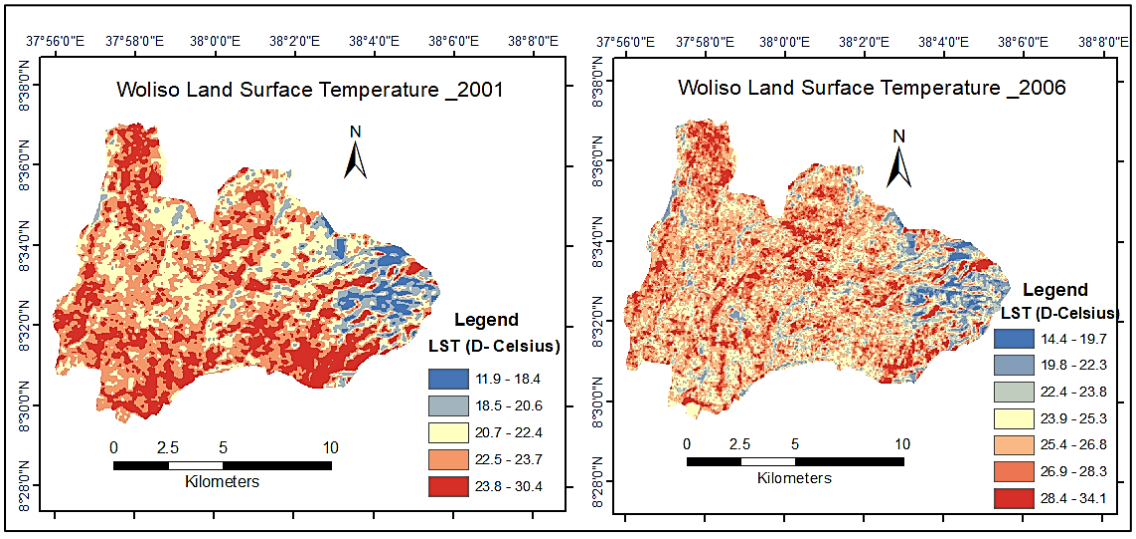

C D

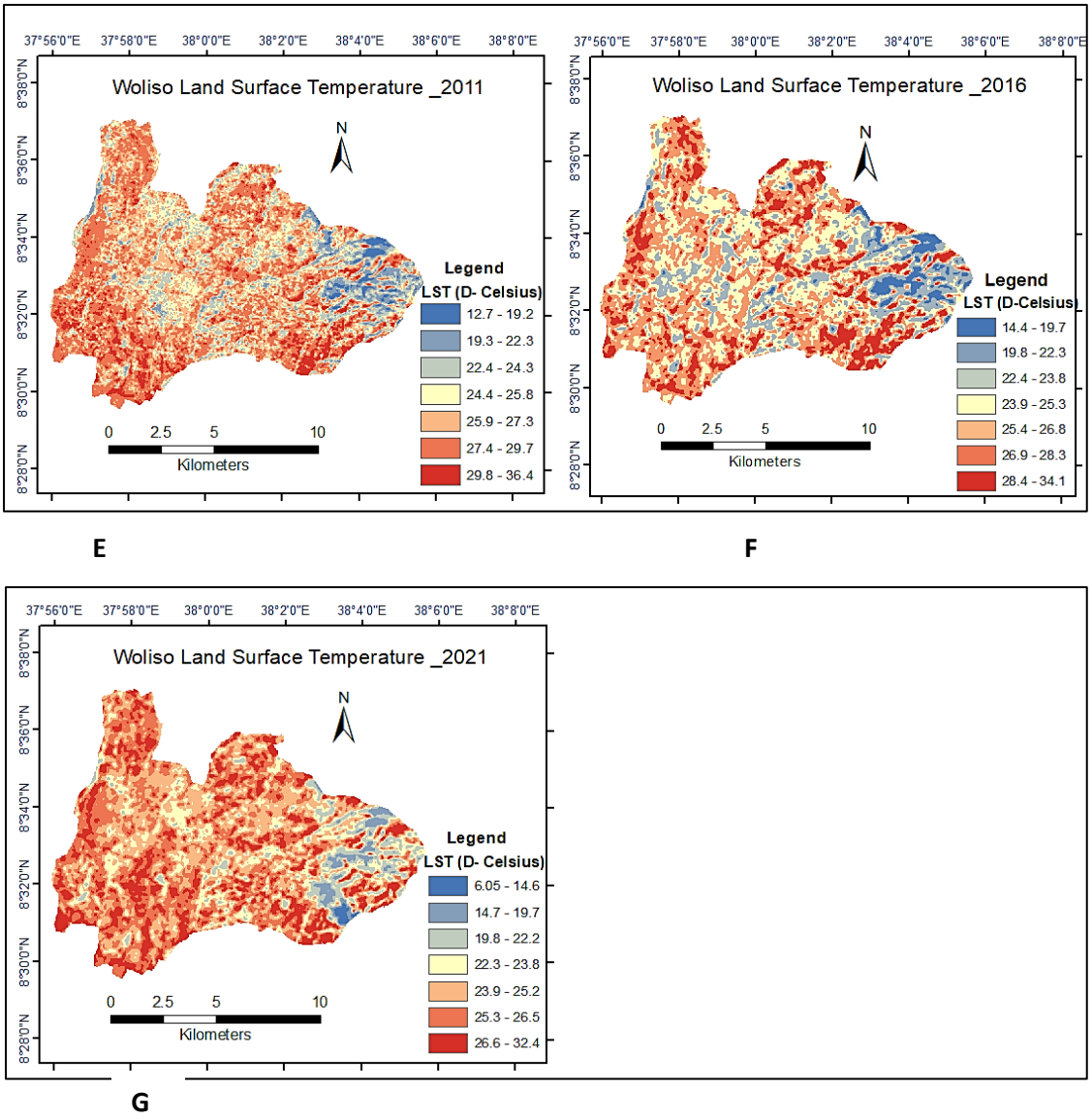

Figure 16: LST map of Woliso Area (1991, 1996, 2001, 2006, 2011, 2016 and 2021)

Table 12: Computation of Minimum, Maximum and Mean LST (◦C) for the study periods

Year	Minimum	Maximum	Mean
1991	11.885	30.83	22.744
1996	13.309	31.646	24.207
2001	11.885	30.42	22.431
2006	14.374	34.067	25.509
2011	12.715	36.384	26.302
2016	14.301	31.798	24.441
2021	6.0545	32.396	24.811

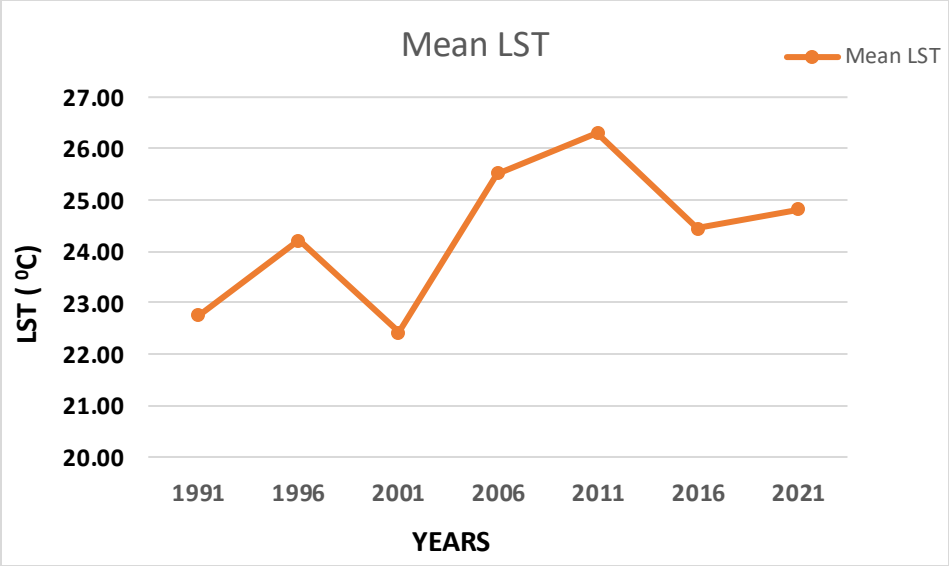

Figure 17: Computation of LST (◦C) for each time interval between 1991 and 2021

4.8. LULC Change and LST

Overall, in this study after the layover of LST maps on the LULC maps, zonal statistics was estimated for the LULC modification. The mean land surface temperature on each LULC classes for all the study years were computed. Consequently, the results of mean LST on agricultural land class was 23.09 °C in 1991 25.82°C in 2006 and 25.03°C in 2021. And on the Builtup area it was 22.91°C in 1991 26.86°C in 2006 and 25.20°C in 2021. The mean LST on dry bare land class was 23.39°C in 1991 25.73°C in 2006 and 25.30°C in 2021, whereas the forest land reveled 20.80°C in 1991 22.74°C in 2006 and 22.86°C in 2021. Finally, the mean LST on wet grass land class was 24.35°C in 1991 27.78°C in 2006 and 26.28°C in 2021 then.

The result of the study also indicated that in line with (Imran et al., 2021) gradual increase of LST was found for all land covers over the study period from 1991 to 2021 irrespective of land cover type., which was the evidence of urban microclimate warming effect in the study area. In consistent with the (Balew and Korme, 2020) LST pattern was changed with the variation of LULC. Accordingly, it was observed that the land surface temperature amplified at elevated rate in those regions wherever the LULC categories were transformed to settlement and bare land. In Built-up classified area and bare land classified area, the surface temperature increased by nearly 2.29°C and 1.91°C respectively. The lowest LST among all LULC classifications is observed in forest land classification during 1991 which scattered in 2021. Overall, the LST scale of forest land areas raised by 2.06°C from 1991 to 2021 in Woliso area during the 30

years period. In agricultural land classified areas, an increase of 1.94°C is observed i.e., the LST value estimated is 23.09°C in 1991 whereas reached 25.03°C in 2021.

The grassland classified areas among all LULC classifications exhibited the higher LST besides an increase from 24.35°C in 1991 to 26.28°C in 2021 was observed. The grassland classified areas showed the higher LST compared to bare land and was that most of the grassland were located at lower elevation between 1950 to 2310 above mean sea level almost whereas more of dry bare landscape located at higher elevation between 2310 to 2770 above mean sea level (contour map annex 3 part of the appendix part). In other words, land surface temperature is dependent on elevation difference, i.e., as altitude increase LST decrease and vice versa. Statistical description of LST in 1991, 2006 and 2021 over different LULC presented below in Table 13 whereas Figure 17 illustrates comparisons of mean LST in different LULC classes during these study period.

Table 13: Statistical description of LST in 1991, 2006 and 2021 over different LULC

LULC Class	Mean LST (°C)			Mean LST Difference (°C)		
	1991	2006	2021	2006 - 1991	2021 - 2006	2021 - 1991
Agricultural Land	23.09	25.82	25.03	2.73	-0.79	1.94
Built-up Area	22.91	26.86	25.2	3.95	-1.66	2.29
Dry bare Land	23.39	25.73	25.3	2.34	-0.43	1.91
Forest Land	20.80	22.74	22.86	1.94	0.12	2.06
Wet Grassland	24.35	27.78	26.28	3.43	-1.5	1.93

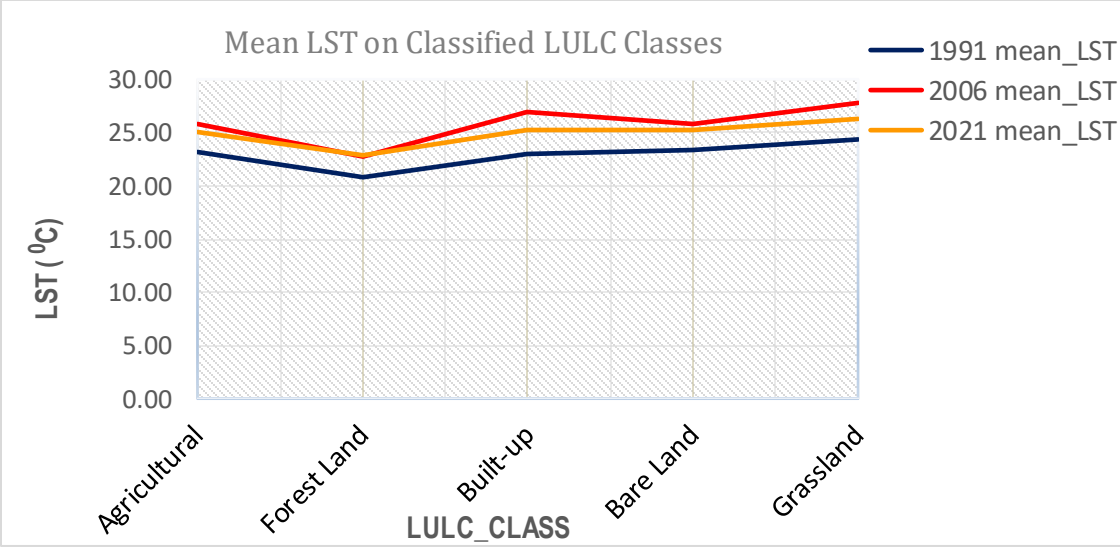

Figure 18: Comparisons of mean LST in different LULC classes during the study period

4.9. Correlation between LST and NDVI

To investigate the correlation between LST and NDVI, regression analysis was carried out for the selected LULC classes. The 5-year interval of NDVI from 1991-2021 was computed with the correlation results in Figure 18. As documented in the most literature, (Nzoiwu et al., 2017; Aboelnour and Engel, 2018; Begum et al., 2021) higher levels of NDVI were associated with lower values of LST. Similarly, the relationship between the LST and NDVI is a negative correlation such that as the NDVI value decreases the LST increase within the study area. The strong negative correlation of NDVI with LST (as illustrated on correlation analysis results bellow Figure 18 with correlation equation and R^2 value) indicates that healthy green vegetation lowers the land surface temperature. The results confirm that high surface temperature was observed in built-up and bare-land surfaces whereas low surface temperatures are in green vegetated areas.

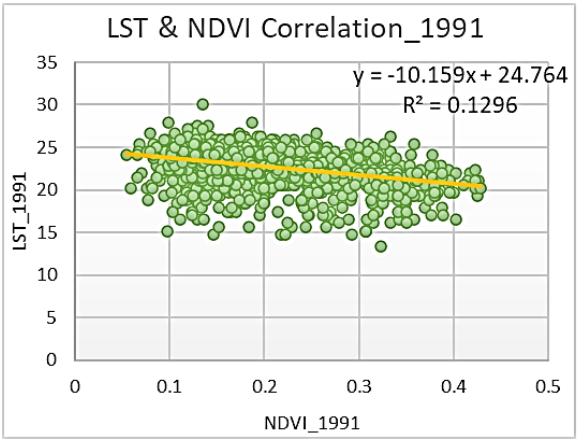

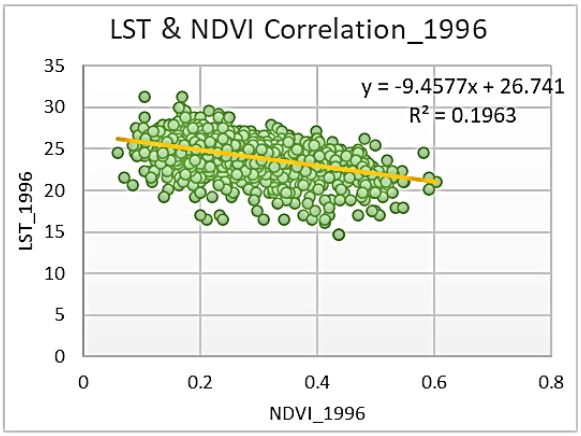

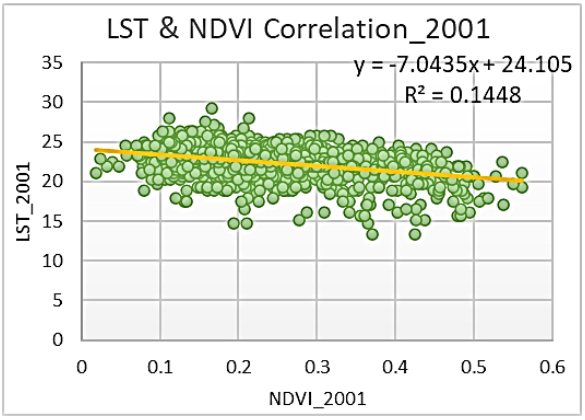

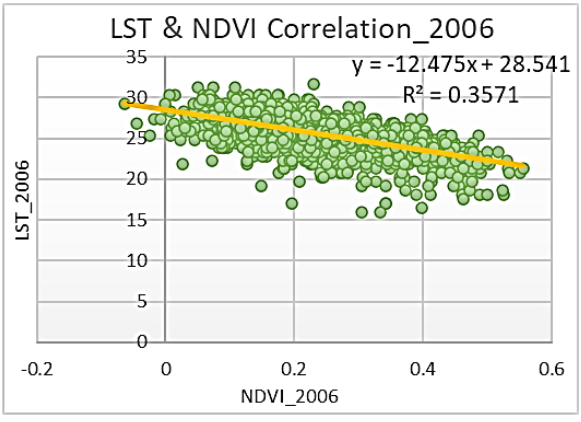

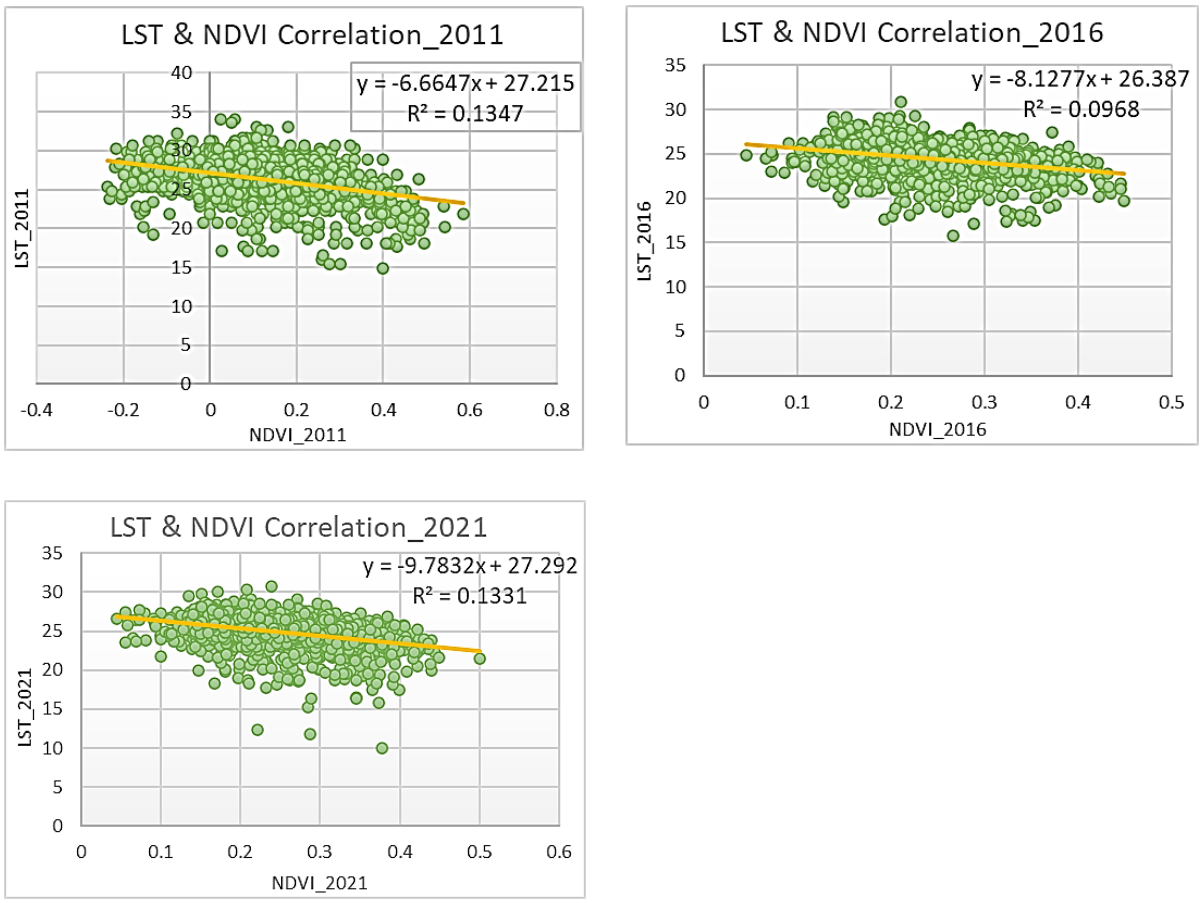

Figure 19: LST and NDVI correlation for years 1991, 1996, 2001, 2011, 2016 and 2021

4.10. Correlation between LST and NDBI

Similar to that of NDVI to investigate the correlation between LST and NDBI, regression analysis was carried out for selected LULC classes. The results of the regression analysis between LST and NDBI are presented in Figure 19 indicating a strong positive linear correlation (as illustrated on correlation analysis results bellow Figure 28 with correlation equation and R2 value) for all the years, with most years depicting correlation between LST and NDBI. This implies that as more buildings are constructed, the density of NDBI increases and the LST also increases which is in line with the works of (Aboelnour and Engel, 2018; Suriana, Barkey and Gou, 2020). The positive relationship between NDBI and LST indicates that built-up area is generating more heat into the environment.

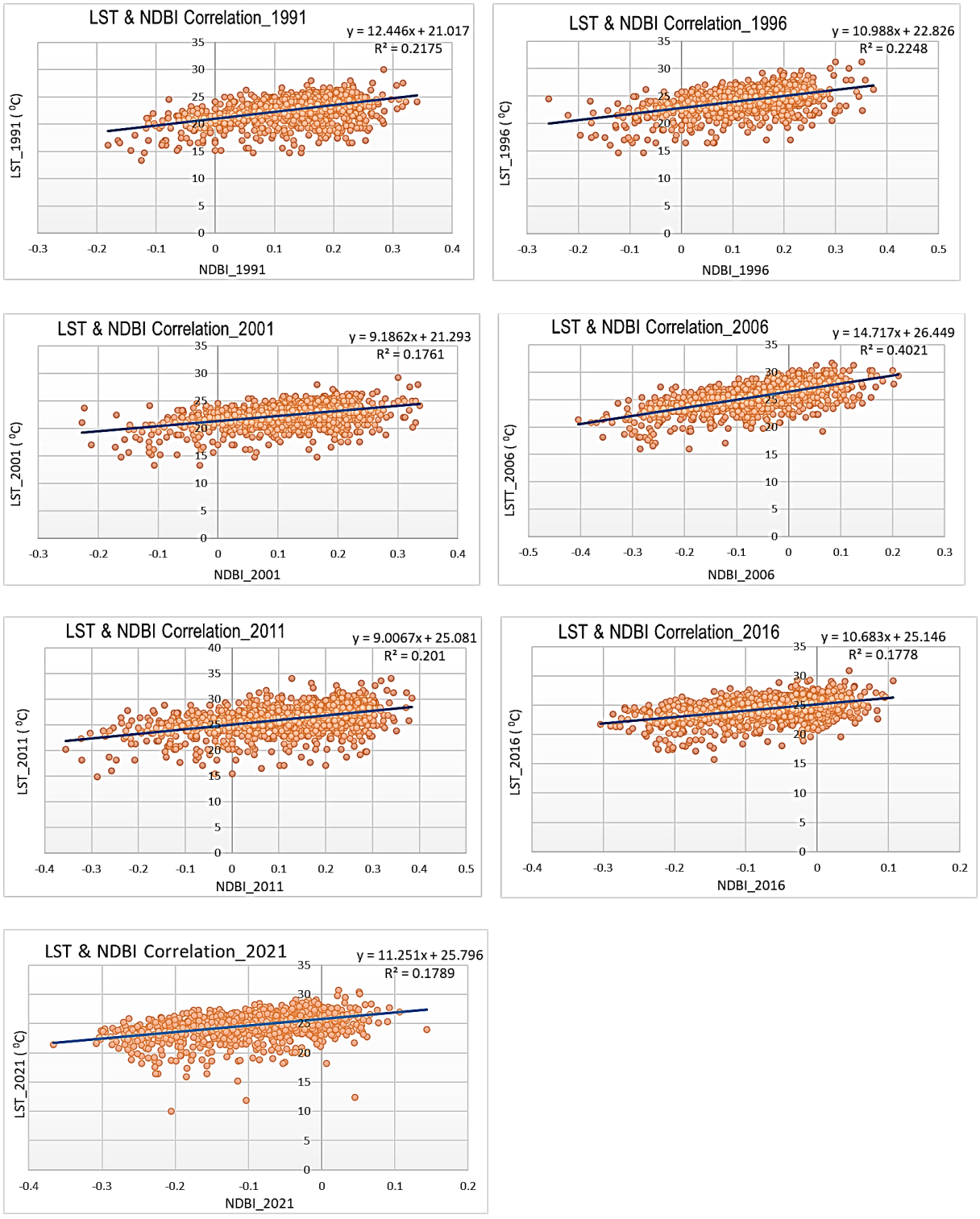

Figure 20: LST and NDVI correlation for years 1991, 1996, 2001, 2011, 2016 and 2021

The correlational results in Figure 18 and Figure 19 confirms that NDBI is higher in areas with high LST, while NDVI is higher in areas with lower LST.

CHAPTER FIVE:

5. CONCLUSION AND RECOMMENDATIONS

Conclusion

This study investigated the impact of land use and land cover changes on urban fringes agriculture and LST from 1991 to 2021 in Woliso town and its surrounding of Oromia Regional State. The freely accessible Landsat satellite image data the best suitable collection two level one (Landsat 5 TM, Landsat 7 ETM^{+} and Landsat 8 OLI/TIRS) for the years 1991, 1996, 2001, 2006, 2011, 2016 and 2021 were obtained from the USGS official website and used. The 1991, 2006 and 2021 accessed image data was used for LULC classification and change detection analysis, whereas all the accessed image data was used for LST retrieval and analysis, NDVI and NDBI calculations and correlation analysis. Besides, to evaluate the impacts of urban sprawl and land use dynamics on urban fringes agriculture; socio-economic data was used.

LULC classification result of 1991 showed that the dominant LULC classes were agricultural land and forest land. These classes accounted for 9492.76 hectares and 2514.25 hectares of the overall area coverage of 13793.6 hectares respectively. The wet grassland accounted 807.1 hectares. However, the Built-up area were 691.2 hectares whereas dry bare land were 288.5 hectares. In 2021 the agricultural land, wet grassland as well as forest land became diminished from the 1991 classification results. In contrary to these the built-up area and dry bare land showed drastic increment. Agricultural land accounted 8582.78 hectares, forest land 1825.06 hectares as well as wet grass land 277.06 hectares of the total coverage consequently. The built-up area was recorded to be 1795.82 hectares where as dry bare land was 1312.78 hectares.

The study revealed that conversions of land from agriculture to urban land represent the most prominent land cover change due to urban expansion and sprawl. In the year 1991 to 2006 about 585.9 hectares of agricultural land was converted to the built-up area where as from 1991 to 2021 about 1186.47 hectares was converted to built-up area. Equally, about 160.99 hectares of wet and grassland in the year 1991 to 2021 were converted to the built-up area. due to rapid prevalence of urban sprawl and other settlement area, primary forests have been affected. In the study area about 100.19 hectares of forest lands were converted to the built-up area in 30-year intervals. In contrary to this only minimal quantity of dry and bare land was converted to the built-up area showing rapid urbanization was consuming valuable land spaces.

The agricultural land class appeared as being maintained in 1991 to 2006 and seemed more change from 2006 to 2021; but it was at the expense of other LULC classes. About 453.63 hectares of wet grassland and about 1262.79 hectares of forest lands were converted to the agricultural land from 1991 to 2021. The forest area was calculated with approximation showing periodic decrement in the study period. But the reality was that substantial quantity of agricultural land was converted to eucalyptus tree plantation and **khat** (local name chaat) production showing the spectral reflectance band as forest land which implies the prevalence of extreme distraction on natural forests.

It was evidenced that the rapid growth of the town has been accompanied with rapid urban population growth and urban sprawling, leading to the incorporation of the half part of the four rural districts in the peri-urban of the town. This significantly affect the size of the total cultivable land for crop production. Concerning the socio-economic influences posed, the impact of urban expansion on the agricultural land as land is the most important economic base for the rural residents is more of pressing. The main problem for the local people as reflected in the FGD, is that most farmers used to earn their livelihoods from their own farm lands and hence, those who lack the skill to join non-farm businesses feared their livelihoods will may worsen finally. Surprisingly, most of the converted lands were for urban residential housing establishments and have not created job opportunity for the affected group.

The successive spatiotemporal Pattern of NDVI and NDBI also showed generally the presence of LULC transformation. AS larger NDVI values indicate more vigorous green vegetation cover; it was revealed that the vegetation cover showed successive and steady decrement from 1991 to 2021 since the maximum positive value showed stepwise decrement per the study years. With the expression (1-NDVI) computed it was implied that by way of gradual decrement in vegetation indicis there is the existence of steady increment in built-up area and barren land. The NDBI value showed almost fluctuating results due to different reasons that need further study in Woliso area.

The spatial distribution of maximum and mean LST experienced oscillation with incremental trend while the overall trend of maximum and mean LST showed positive increase of 1.56^0C, 2.07^0C during the total study period respectively. The gradual increase of LST was found for all land covers over the study period irrespective of land cover type but it was observed that

the LST amplified at elevated rate in regions where the LULC categories were transformed to built-up and bare land. In built-up area and dry bare land classified area, the LST was increased by nearly 2.29°C and 1.91°C respectively. The lowest LST among all LULC class was observed on forest land class during the 30 years period. The grassland classified areas exhibited higher LST compared to bare land and was that most of the grassland were located at lower elevation whereas more of dry bare landscape located at higher elevation above mean sea level.

Finally, the regression analysis between LST and NDVI carried out for the selected LULC classes showed that relationship between LST and NDVI has a negative correlation such that as the NDVI value decreases the LST increase within the study period. The strong negative correlation of NDVI with LST indicates that healthy green vegetation lowers the LST. The results confirm that high surface temperature was observed in built-up and bare-land surfaces whereas low surface temperatures are in green vegetated areas. On the other hand, the correlation analysis between LST and NDBI showed strong positive linear correlation for all the years, with most years depicting correlation between LST and NDBI. This implies that as more buildings are constructed, the density of NDBI increases and the LST also increases.

Recommendations

The emphasis of this study was to assess and examine the impacts of land use and land cover changes on urban fringes agriculture and LST from 1991 to 2021 in Woliso town. The study revealed and showed that LULC change has considerable impacts on urban fringes agriculture and LST on the study area. Therefore, based on the results and findings revealed the following recommendations have drawn.

- LULC change becomes a vital element in current strategies for managing resources and monitoring environmental changes. Therefore, the governmental and non-governmental bodies should give high attention for proper land-use management and socioeconomic effect of LULC change.
- Land managers and environmental experts should control LULC changes through different measures to minimize the influence on the environments and LST.
- Improve the land management knowledge and skills of the city planners to balance the increasing land demand and the loss of agricultural land.

- The city is expanding horizontally and its impact is clear. Hence, the planners should consider vertical development of the town, should make a proper plan for environment-friendly construction, green building, and green/cool roof technology.
- The city has to thoroughly and economically use existing land stock within its planning borderline before acquiring additional land from nearby rural areas. The legal acquisition of fringe land should be based on scientific predictions, and once the land is acquired proper inventory should be kept and well managed to avoid urban sprawl at urban fringe.
- Future compulsory land acquisition plans should consider the livelihood of the affected community, and the environmental and economic contribution of agriculture.
- The method of land valuation and amount of compensation has to consider current land market condition and cost of living. Hence the existing valuation and compensation laws need to be revised in a manner to reflect these,
- The urban administration needs to establish rehabilitation programs to support expropriated farmers. The support programs may include skill training, financial planning advice, business building support, providing plots to run business among others.
- The output of this research can serve as an input for future researchers who want to study the impact of LULC changes on economic, social and environmental issues.

Reference

Aboelnour, M. and Engel, B.A. (2018) 'Application of Remote Sensing Techniques and Geographic Information Systems to Analyze Land Surface Temperature in Response to Land Use / Land Cover Change in Greater Cairo Region ', pp. 57–88. doi:10.4236/jgis.2018.101003.

Anwar, H.M.I. *et al.* (2021) 'Impact of Land Cover Changes on Land Surface Temperature and Human Thermal Comfort in Dhaka City of Bangladesh', *Journal of Earth Systems and Environment*, 5(3), pp. 667–693. doi:10.1007/s41748-021-00243-4.

Artis, D.A. and Carnahan, W.H. (1982) 'Survey of emissivity variability in thermography of urban areas', *Elsevier Science Publishing Co., Remote Sensing of Environment*, 12(4), pp. 313–329. doi:10.1016/0034-4257(82)90043-8.

Avdan, U. and Jovanovska, G. (2016) 'Algorithm for Automated Mapping of Land Surface Temperature Using LANDSAT 8 Satellite Data', *Hindawi Publishing Corporation; Journal of Sensors*, 2016, pp. 1–9. doi:10.1155/2016/1480307.

Balew, A. and Korme, T. (2020) 'Monitoring land surface temperature in Bahir Dar city and its surrounding using Landsat images', *The Egyptian Journal of Remote Sensing and Space Sciences*, 23(3), pp. 371–386. doi:10.1016/j.ejrs.2020.02.001.

Ban, Y. (2016) *Remote Sensing and Digital Image Processing Volume 20 EARSeL Series Editor*. Springer International Publishing. doi:10.1007/978-3-319-47037-5.

Begum, M.S. *et al.* (2021) 'An Analysis of Spatio-Temporal Trends of Land Surface Temperature in the Dhaka Metropolitan Area by Applying Landsat Images', *Journal of Geographic Information System*, pp. 538–560. doi:10.4236/jgis.2021.134030.

Belay, E. (2014) 'Impact of Urban Expansion on the Agricultural Land Use a Remote Sensing and GIS Approach : A Case of Gondar City , Ethiopia', *International Journal of Innovative Research & Development*, 3(6), pp. 129–133.

Blaschke, T. (2010) 'Object based image analysis for remote sensing', *ISPRS Journal of Photogrammetry and Remote Sensing*, 65(1), pp. 2–16. doi:10.1016/j.isprsjprs.2009.06.004.

Bonafoni, S. and Sekertekin, A. (2020) 'Land Surface Temperature Retrieval from Landsat 5, 7, and 8 over Rural Areas: Assessment of Different Retrieval Algorithms and Emissivity Models and Toolbox Implementation', *MDPI_journal Remote Sensing*, (294), pp. 1–32. doi:10.3390/rs12020294.

Boori, M.S. *et al.* (2015) 'Monitoring and modeling of urban sprawl through remote sensing and GIS in Kuala', *a SpringerOpenJournal* [Preprint]. doi:10.1186/s13717-015-0040-2.

Campbell, J.B. (2011) *Introduction to remote sensing / James B. Campbell, Randolph H. Wynne. — 5th ed.* The Guilford Press A Division of Guilford Publications, Inc. 72 Spring Street, New York, NY 10012 www.guilford.com.

Canty, M.J. (2009) *Image Analysis, Classification, and Change Detection in Remote Sensing; with Algorithms for ENVI/IDL*. Second Ed. CRC Press, Taylor & Francis Group.

Canty, M.J. (2014) *Image Analysis, Classification and Change Detection in Remote Sensing*. 3 rd. Ed., *CRC Press*. 3 rd. Ed. CRC Press; Taylor & Francis Group. doi:10.1201/b17074.

Chapin, F.S. *et al.* (2005) 'Role of Land-Surface Changes in Arctic Summer Warming', *sciencemag.org*, 310, pp. 657–660. doi:10.1126/science.1116349.

Congalton, R.G. *et al.* (2017) *Imagery and GIS : best practices for extracting information from imagery /*. Esri Press, 380 New York Street, Redlands, California 92373-8100.

CSA (2022) 'Ethiopian 2022 Project Population Census', (July), p. 13.

Dadi, D. *et al.* (2018) 'Urban sprawl and its impacts on land use change in Central Ethiopia Urban Forestry & Urban Greening Urban sprawl and its impacts on land use change in Central Ethiopia', *Urban Forestry & Urban Greening*, 16(March), pp. 132–141. doi:10.1016/j.ufug.2016.02.005.

Darrin, B. and Kaminiski, V. (2016) *Urban Studies and Sprawl (concepts , Elements and Issues) Revised Edition: 2016*. Academic Studio 48 West 48 Street, Suite 1116, New York, NY 10036, United States.

Dejene, A. (2016) 'School of Graduate Studies College of Social Sciences Impactof Urban Sprawlon Farm Lands: the Case Ofsebeta Town, Central Ethiopia Dejene Adugna a Thesis Submitted To the Department of Geography and Environmental Studies Presented in Partial

Fulfillment o', *Addis Ababa University School of Graduate Studies* [Preprint], (June).

Deribew, K.T. (2020) 'Spatiotemporal analysis of urban growth on forest and agricultural land using geospatial techniques and Shannon entropy method in the satellite town of Ethiopia, the western fringe of Addis Ababa city', *Ecological Processes*, 9(1). doi:10.1186/s13717-020-00248-3.

Dessu, T. *et al.* (2020) 'Long-Term Land Use Land Cover Change in Urban Centers of Southwest Ethiopia From a Climate Change Perspective', *Front. Clim. 2:577169*, 2, pp. 1–23. doi:10.3389/fclim.2020.577169.

Dissanayake, D. (2020) 'Land Use Change and Its Impacts on Land Surface Temperature in Galle City , Sri Lanka', *MDPI_climate*, (65), pp. 1–15. doi:doi:10.3390/cli8050065.

Dodd, E., Veal, K. and Ghent, D. (2016) 'Satellite LST User Handbook WP3.4 – DEL-25', *GlobTemperature Consortium;Organisation: ULeic, ESA,* GlobT-WP3-.

Du, C. *et al.* (2015) 'A Practical Split-Window Algorithm for Estimating Land Surface Temperature from Landsat 8 Data', pp. 647–665. doi:10.3390/rs70100647.

Duro, D.C. (2012) 'Remote Sensing and Gis in Support of Sustainable Agricultural Development', *Degree of Doctor of Philosophy in the School of Environment and Sustainability / University of Saskatchewan*, (March 2012), p. 191.

Fabeku, B.B. *et al.* (2018) 'Spatio-Temporal Variability in Land Surface Temperature and Its Relationship with Vegetation Types over Ibadan, South-Western Nigeria', *Atmospheric and Climate Sciences*, 08(03), pp. 318–336. doi:10.4236/acs.2018.83021.

Fitawok, M.B. *et al.* (2020) 'Modeling the Impact of Urbanization on Land-Use Change in Bahir Dar City, Ethiopia: An Integrated Cellular Automata–Markov Chain Approach', *mdpi_land*, pp. 1–17. doi:10.3390/land9040115.

Fonseka, H.P.U. *et al.* (2016) 'Urbanization and Its Impacts on Land Surface Temperature in Colombo Metropolitan Area , Sri Lanka , from 1988 to 2016', *MDPI_remote sensing*, pp. 1–18. doi:doi:10.3390/rs11080957.

Foody, G. (2010) *Assessing the Accuracy of Remotely Sensed Data: Principles and Practices*, *The Photogrammetric Record*. doi:10.1111/j.1477-9730.2010.00574_2.x.

Friedel, M.J. (2012) 'Data-driven modeling of surface temperature anomaly and solar activity trends', *Elsevier; Envi/ Modelling & Software*, pp. 1–16. doi:10.1016/j.envsoft.2012.04.016.

García-Santos, J.C.D.M.-V.M.A.J. and G.S. (2018) 'Comparison of Three Methods for Estimating Land Surface Temperature from Landsat 8-TIRS Sensor Data', pp. 1–13. doi:10.3390/rs10091450.

Gashu, K. and Egziabher, T.G. (2018) 'Spatiotemporal trends of urban land use / land cover and green infrastructure change in two Ethiopian cities : Bahir Dar and Hawassa', *Environmental Systems Research* [Preprint], (May). doi:10.1186/s40068-018-0111-3.

Gebregziabher, Z. (2014) 'The Impact of Urban Sprawl on the Livelihood of Fringe Farmers in Mekelle , Ethiopia', *Research on Humanities and Social Sciences;IISTE journals*, 4(16).

Getu, A. (2014) 'ANALYSIS OF URBAN LAND USE AND LAND COVER CHANGES ':, *Universitat Jaume; Geospatial technologies* [Preprint].

Grimm, N.B. *et al.* (2008) 'The changing landscape: Ecosystem responses to urbanization and pollution across climatic and societal gradients', *Frontiers in Ecology and the Environment*, 6(5), pp. 264–272. doi:10.1890/070147.

Guha, S. *et al.* (2020) 'Analytical study on the relationship between land surface temperature and land use /land cover indices', *Annals of GIS*, 26(2), pp. 201–216. doi:10.1080/19475683.2020.1754291.

Halefom, A. *et al.* (2018) 'Dynamics of Land Use and Land Cover Change Using Remote Sensing and GIS : A Case Study of', *Journal of Geographic Information System*, pp. 165–174. doi:10.4236/jgis.2018.102008.

He, C. *et al.* (2010) 'Improving the normalized difference built-up index to map urban built-up areas using a semiautomatic segmentation approach', *Remote Sensing Letters*, 1(4), pp. 213–221. doi:10.1080/01431161.2010.481681.

He, Y. and Weng, Q. (2018) *High Spatial Resolution Remote Sensing: Data, Analysis, and Applications*. CRC Press; Taylor & Francis Group, LLC.

Huang, S. *et al.* (2020) 'A commentary review on the use of normalized difference vegetation index (NDVI) in the era of popular remote sensing', *Journal of Forestry*

Research, 32(1), pp. 1–6. doi:10.1007/s11676-020-01155-1.

Imran, H.M. *et al.* (2021) 'Impact of Land Cover Changes on Land Surface Temperature and Human Thermal Comfort in Dhaka City of Bangladesh', *Earth Systems and Environment*, 5(3), pp. 667–693. doi:10.1007/s41748-021-00243-4.

Indira Gandhi (2012) *REMOTE SENSING AND IMAGE INTERPRETATION*. Maidan Garhi, New Delhi: Indira Gandhi National Open University School of Sciences' IGNOU/SOS.

Jeevalakshmi, D. (2017) 'Land Surface Temperature Retrieval from LANDSAT data using Emissivity Estimation', *International Journal of Applied Engineering Research*, 12(20), pp. 9679–9687.

Jensen, J.R. (2014) *Remote Sensing of the Environment An Earth Resource Perspective / Second Edition*. 2nd Edi. Pearson Prentice Hall; Edinburgh Gate Harlow Essex CM20 2JE.

Jensen, J.R. (2015) *INTRODUCTORY DIGITAL IMAGE PROCESSING: A Remote Sensing Perspective*. 4th editio. University of South Carolina: Pearson series in geographic information science; United States of America.

Jimenez-Munoz *et al.* (2004) 'A generalized single-channel method for retrieving land surface temperature from remote sensing data', *Journal of Geophysical Research*, 108(NO. D22, 4688,). doi:10.1029/2003JD003480.

Jiménez-muñoz, J.C. *et al.* (2014) 'Land Surface Temperature Retrieval Methods From Landsat-8 Thermal Infrared Sensor Data', *IEEE Geoscience and Remote Sensing Letters,* 11(10), pp. 1840–1843.

Kalnay, E. and Cai, M. (2013) 'Impact of Urbanization and Land-Use Change on Climate "Article in Nature · June 2003"', *ResearchGate.net 'Article in Nature · June 2003'*, 423(June 2003), pp. 438–443. doi:10.1038/nature01675.

Karnieli, A. *et al.* (2009) 'Use of NDVI and Land Surface Temperature for Drought Assessment : Merits and Limitations', *JOURNAL OF CL IMATE; American Meteorological Society*, 23, pp. 618–633. doi:10.1175/2009JCLI2900.1.

Kassa, F. (2013) 'Conurbation and Urban Sprawl in Africa : The case of the City of Addis Ababa', *Ghana Journal of Geography*, 5, pp. 73–89.

Kebebew, S., Worku, K. and Babu, A. (2019) 'Spatio-Temporal Analysis of Land Use/Land Cover Change and Urban Sprawl Using GIS and Remote Sensing Technologies : The Case of Laga Tafo-Laga Dadi Town , Oromia , Ethiopia', *Journal of Sciences: Basic and Applied Research*, 4531.

Kemarau, R.A. and Eboy, O.V. (2020) 'Land Coverage Indices and its Impact on Land Surface Temperature Pattern in Small Medium Sizes, Kota Kinabalu City for the Year 1991, 2011 And 2018', *Journal of Built Environment, Technology and Engineering,* 7, pp. 0128–1003. doi:10.51200/jobsts.v6i1.2791.

Kercival, N. (2015) 'Assessing Changes in Land Use and Land Cover using Remote Sensing :A Case Study of the Umhlanga Ridge Sub - Place', *University of KwaZulu-Natal, Durban*, pp. 1–142.

Khorram, S. *et al.* (2016) *Principles of Applied Remote Sensing*. New York: Springer Science Business Media LLC New. doi:DOI 10.1007/978-3-319-22560-9.

Kuenzer, C. and Dech, S. (2013) *Remote Sensing and Digital Image Processing: Thermal Infrared Remote Sensing: Sensors, Methods, Applications*. springer.com. doi:10.1007/978-94-007-6639-6_15.

Li, Y., Zhang, H. and Kainz, W. (2012) 'Monitoring patterns of urban heat islands of the fast-growing Shanghai metropolis , China : Using time-series of Landsat TM / ETM + data', *Journal of Ap/Earth Obs/ and Geoinformation*, pp. 127–138. doi:10.1016/j.jag.2012.05.001.

Lillesand, T. *et al.* (2015) *Remote Sensing and Image Interpretation*. Seventh ed. Edited by R. Flahive and M.P.K.H.C.V.J. Nollen. JohnWiley&Sons, Inc.

Liu, J.G. and Mason, philippa J. (2016) *Image processing and GIS for remote Sensing; Techniques and applications*. Second edI. The atrium, Southern Gate, Chichester, West Sussex, PO19 8SQ, UK Editorial: John Wiley & Sons, Ltd.,.

Liu, J.G. and Mason, P.J. (2009) *Essential Image Processing and GIS for Remote Sensing*. The Atrium, South Gate, Chichester, West Sussex, PO19 8SQ, UK: John Wiley & Sons Ltd.

Lu, D. *et al.* (2004) 'Change Detection Techniques. "Article in International Journal of Remote Sensing · January 2004"', *ResearchGate.net 'International Journal of Remote*

Sensing', 25(20 JUNE), pp. 2365–2407. doi:10.1080/0143116031000139863.

Lu, D. and Weng, Q. (2007) 'A survey of image classification methods and techniques for improving classification performance', *International Journal of Remote Sensing*, 28(5), pp. 823–870. doi:10.1080/01431160600746456.

Lunetta, R.S. and Lyon, J.G. (2004) *Remote Sensing and GIS Accuracy Assessment*. CRC Press LLC, 2000 N.W. Corporate Blvd., Boca Raton, Florida 33431.

Maimaitiyiming, M. *et al.* (2014) 'Effects of green space spatial pattern on land surface temperature : Implications for sustainable urban planning and climate change adaptation', *Elsevier; ISPRS Journal of Photogrammetry and Remote Sensing*, 89, pp. 59–66. doi:10.1016/j.isprsjprs.2013.12.010.

Mallick, J., Kant, Y. and Bharath, B.D. (2008) 'Estimation of land surface temperature over Delhi using Landsat-7 ETM +', *J. Ind. Geophys. Union (*, 12(3), pp. 131–140.

McFeeters, S.K. (1996) 'The use of the Normalized Difference Water Index (NDWI) in the delineation of open water features', *International Journal of Remote Sensing*, 17(7), pp. 1425–1432. doi:10.1080/01431169608948714.

Mcmillin, L.M. (1975) 'Estimation of Sea Surface Temperatures from Two Infrared Window Measurements with Different Absorption', *Journal of Geophysical Research*, 80(36), pp. 5113–5117.

Mekuriaw, T. (2019) 'The Impact of Urban Expansion on Physical Environment in', *Civil and Environmental Research*, 11(5), pp. 16–26. doi:10.7176/CER.

Mohan, M. *et al.* (2011) 'Dynamics of Urbanization and Its Impact on Land-Use/Land-Cover: A Case Study of Megacity Delhi', *Journal of Environmental Protection*, 02(09), pp. 1274–1283. doi:10.4236/jep.2011.29147.

Nzoiwu, C.P. *et al.* (2017) 'Impact of Land Use / Land Cover Change on Surface Temperature Condition of', *Journal of Geographic Information System*, pp. 763–776. doi:10.4236/jgis.2017.96047.

Olofsson, P. *et al.* (2014) 'Good practices for estimating area and assessing accuracy of land change', *Remote Sensing of Environment*, 148, pp. 42–57. doi:10.1016/j.rse.2014.02.015.

Ouma et al., Y. (2021) 'Urban land surface temperature variations with LULC, NDVI and NDBI in semi-arid urban environments: case study of Gaborone City, Botswana (1989–2019)', in *Proc. SPIE 11864, Remote Sensing Technologies and Applications in Urban Environments VI, 1186409 (12 Sep 2021);* SPIEDigitalLibrary. doi:10.1117/12.2595031.

Pettorelli, N. *et al.* (2005) 'Using the satellite-derived NDVI to assess ecological responses to environmental change', *Trends in Ecology and Evolution*, 20(9), pp. 503–510. doi:10.1016/j.tree.2005.05.011.

Pradhan, B. (2017) *Spatial Modeling and Assessment of Urban Form_Analysis of Urban Growth: From Sprawl to Compact Using Geospatial Data*. Serdang, Malaysia: Springer International Publishing. doi:10.1007/978-3-319-54217-1.

Qin, Z. *et al.* (2001) 'A mono-window algorithm for retrieving land surface temperature from Landsat TM data and its application to the Israel-Egypt border region', *International Journal of Remote Sensing*, 22(18), pp. 3719–3746. doi:10.1080/01431160010006971.

Rahman, M.T. (2016a) 'Detection of land use/land cover changes and urban sprawl in Al-Khobar, Saudi Arabia: An analysis of multi-temporal remote sensing data', *ISPRS International Journal of Geo-Information*, 5(2). doi:10.3390/ijgi5020015.

Rahman, M.T. (2016b) 'Detection of Land Use / Land Cover Changes and Urban Sprawl in Al-Khobar , Saudi Arabia : An Analysis of Multi-Temporal Remote Sensing Data', *I/J/ Geo-Information*, pp. 1–17. doi:10.3390/ijgi5020015.

Rasul, G. and Ibrahim, F. (2017) 'Urban Land Use Land Cover Changes and Their Effect on Land Surface Temperature : Case Study Using Dohuk City in the Kurdistan Region of Iraq', *MDPI/climate*, pp. 1–18. doi:10.3390/cli5010013.

REF (2021) *Research and Evidence Facility (REF): 'Rural-urban migration , urban informality and the challenges of promoting inclusive development in Ethiopia'*. London: EU Trust Fund for Africa (Horn of Africa Window) Research and Evidence Facility.

Richards J (1999) *Remote Sensing Digital Image Analysis*. Third Edit. Springer-Verlag Berlin Heidelberg. doi:10.1007/978-3-662-03978-6.

Rousta, I. *et al.* (2018) 'Spatiotemporal Analysis of Land Use / Land Cover and Its Effects on

Surface Urban Heat Island Using Landsat Data : A Case Study of Metropolitan City', *MDPI_sustainability* [Preprint]. doi:10.3390/su10124433.

Rozenstein, O. *et al.* (2014) 'Derivation of Land Surface Temperature for Landsat-8 TIRS Using a Split Window Algorithm', *MDPI/ Sensors*, (June), pp. 5768–5780. doi:10.3390/s140405768.

Samanta, S. and Pal, D.K. (2016) 'Change Detection of Land Use and Land Cover over a Period of 20 Years in Papua New Guinea', *Natural Science*, 8(March), pp. 138–151. doi:10.4236/ns.2016.83017 Change.

Simbangala, M.S. *et al.* (2015) 'Using object-oriented image analysis to map and monitor land cover change in the Region Costa Maya , México 1993-2010', *Investig. Geogr*, 50, pp. 33–50.

Singh, A. (1989) 'Review Articlel: Digital change detection techniques using remotely-sensed data', *International Journal of Remote Sensing,* 10(6), pp. 989–1003. doi:10.1080/01431168908903939.

Sobrino, J.A. *et al.* (2004) 'Land surface temperature retrieval from LANDSAT TM 5', *Remote Sensing of Environment*, 90(4), pp. 434–440. doi:10.1016/j.rse.2004.02.003.

Suriana, D., Barkey, R.A. and Gou, Z. (2020) 'Analysis of Land Use / Land Cover Change And Their Effects On Spatiotemporal Patterns Of Urban Heat Islands (UHI) In The City Of Makassar , Indonesia', *International Journal of Engineering and Science Application*, 7(2).

Terfa, B.K. *et al.* (2017) 'Urban Expansion in Ethiopia from 1987 to 2017 : Characteristics , Spatial Patterns , and Driving Forces', *MDPI/ sustainability*, pp. 1–21. doi:10.3390/su11102973.

Tesfaunegn, E.A. (2017) *Urban and Peri- Urban Development Dynamics in Ethiopia: Study for Swiss Agency for Development and Cooperation*. Addis Ababa; Ethiopia.

Thenkabail, P. and Lyon, J. (2009) 'Remote Sensing of Global Croplands for Food Security', in Prasad S. Thenkabail, John G. Lyon, H.T.C.M.B. (ed.). CRC Press ;Taylor & Francis Group, pp. 461–466. doi:10.1201/9781420090109.sec8.

Thenkabail, P.S. (2016a) *REMOTE SENSING HANDBOOK VOLUME I: Remotely Sensed*

Data Characterization, Classification, and Accuracies. USGS: Taylor & Francis Group.

Thenkabail, P.S. (2016b) *REMOTE SENSING HANDBOOK VOLUME II: Land Resources Monitoring, Modeling, and Mapping*. USGS: Taylor & Francis Group.

Thenkabail, P.S. (2016c) *REMOTE SENSING HANDBOOK VOLUME III: Remote Sensing of Water Resources, Disasters, and Urban Studies*. USGS: Taylor & Francis Group.

UN-HABITAT (2008) *ETHIOPIA URBAN PROFILE*. Edited by T.T. and C.G. Semu. Nairobi, Kenya: UN-HABITAT Regional and Technical Cooperation Division.

United Nations (2009) *World Urbanization Prospects The 2009 Revision Highlights*, *Department of Economic and Social Affairs, Population Division*. New York,: UN,.

United Nations (2019) *World Urbanization Prospects; The 2018 Revision*, *Department of Economic and Social Affairs, Population Division*. New York,: United Nations.

USGS (2019a) *Landsat 7 (L7) Data Users Handbook*. U.S.G.S., Department of the Interior. Available at: https://d9-wret.s3.us-west-2.amazonaws.com/assets/palladium/production/s3fs-public/atoms/files/LSDS-1927_L7_Data_Users_Handbook-v2.pdf.

USGS (2019b) *Landsat 8 (L8) Data Users Handbook*. U.S.G.S., Department of the Interior. Available at: https://d9-wret.s3.us-west-2.amazonaws.com/assets/palladium/production/s3fs-public/atoms/files/LSDS-1574_L8_Data_Users_Handbook-v5.0.pdf.

Viana, C.M. *et al.* (2019) *Spatial Modeling in GIS and R for Earth and Environmental Sciences: Land Use/Land Cover Change Detection and Urban Sprawl Analysis*. LISBON: Candice Janco Elsevier publications; doi:10.1016/B978-0-12-815226-3.00029-6.

Wadduwage, S. *et al.* (2017) 'Agricultural land fragmentation at urban fringes: Application of urban-to-rural gradient analysis in Adelaide', *mdpi_Land*, 6(2). doi:10.3390/land6020028.

Wadduwage, S. (2018) 'Peri-urban agricultural land vulnerability due to urban sprawl–a multi-criteria spatially-explicit scenario analysis', *Journal of Land Use Science*, 13(3), pp. 358–374. doi:10.1080/1747423X.2018.1530312.

Walawender, J., Hajto, M. and Iwaniuk, P. (2012) 'A new ArcGIS toolset for automated mapping of Land surface Temperature with the use of LANDSAT satellite data', in *Proc.*

IEEE International Geoscience and Remote Sensing Symposium (IGARSS), 22-27 July 2012, Munich, Germany, pp. 4371–4374. doi:10.1109/IGARSS.2012.6350405.

Wang, F. *et al.* (2015) 'An improved mono-window algorithm for land surface temperature retrieval from landsat 8 thermal infrared sensor data', *MDPI/ Remote Sensing*, 7(4), pp. 4268–4289. doi:10.3390/rs70404268.

Wang, L., Lu, Y. and Yao, Y. (2019) 'Comparison of Three Algorithms for the Retrieval of Land Surface Temperature from Landsat 8 Images', *MDPI ; Journal of Sensors*, (5049), pp. 1–22. doi:10.3390/s19225049.

Weng, Q. (2008) *Remote sensing of impervious surfaces / edited by Qihao Weng. p.* Indiana State University, Terre Haute, Indiana, U.S.A: CRC Press -Taylor & Francis Group 6000.

Wilson, B. and Chakraborty, A. (2013) 'The environmental impacts of sprawl: Emergent themes from the past decade of planning research', *Sustainability (Switzerland)*, 5(8), pp. 3302–3327. doi:10.3390/su5083302.

World Bank (2011) *From Farm to Firm; Rural-Urban Transition in Developing Countries*. Edited by N. Dudwick et al. N Y,: The World Bank Group. doi:10.5860/choice.49-2189.

World Bank (2015) *The Ethiopia Urbanization Review: Urban Institutions for a Middle-Income Ethiopia*, *World Bank Group_Cities Alliance: Cities Without Slums*. Addis Ababa.

Wu, J. (2008) 'The magazine of food, farm, and resource issues Land Use Changes: Economic, Social, and Environmental Impacts', *CHOICES: The magazine of food,farm, and resource issues A publication of the Agricultural & Applied Economics Association*, 23(4).

Yesserie, A.G. (2009) 'SPATIO-TEMPORAL LAND USE/LAND COVER CHANGES ANALYSIS AND MONITORING IN THE VALENCIA MUNICIPALITY, SPAIN', *Universitat Jaume; Geospatial technologies* [Preprint].

Yesuph, A.Y. and Dagnew, A.B. (2019) 'Land use / cover spatiotemporal dynamics , driving forces and implications at the Beshillo catchment of the Blue Nile Basin , North Eastern Highlands of Ethiopia', *Environmental Systems Research* [Preprint]. doi:10.1186/s40068-019-0148-y.

Zhang, Q., Schaaf, C. and Seto, K.C. (2013) 'The Vegetation adjusted NTL Urban Index: A

new approach to reduce saturation and increase variation in nighttime luminosity', *Remote Sensing of Environment*, 129, pp. 32–41. doi:10.1016/j.rse.2012.10.022.

Zhao, H. *et al.* (2020) 'Spatiotemporal Characteristics of Urban Surface Temperature and Its Relationship with Landscape Metrics and Vegetation Cover in Rapid Urbanization Region', *WILEY ; Hindawi*, 2020. doi:https://doi.org/10.1155/2020/7892362.

Appendixes

Annex 1: Specification of Landsat Image Bands

Specification of Landsat image bands

Satellite	Band	Wavelength (μm)	Resolution (m)
Landsat-5 TM (Thematic Mapper)	Band 1—Blue	0.45–0.52	30
	Band 2—Green	0.52–0.60	30
	Band 3—Red	0.63–0.69	30
	Band 4—Near Infrared (NIR)	0.76–0.90	30
	Band 5—Shortwave Infrared (SWIR) 1	1.55–1.75	30
	Band 6—Thermal	10.40–12.50	120* (30)
	Band 7—Shortwave Infrared (SWIR) 2	2.08–2.35	30
Landsat-7 ETM + (Enhanced Thematic Mapper Plus)	Band 1—Blue	0.45–0.52	30
	Band 2—Green	0.52–0.60	30
	Band 3—Red	0.63–0.69	30
	Band 4—Near Infrared (NIR)	0.77–0.90	30
	Band 5—Shortwave Infrared (SWIR) 1	1.55–1.75	30
	Band 6—Thermal	10.40–12.50	60* (30)
	Band 7—Shortwave Infrared (SWIR) 2	2.09–2.35	30
	Band 8—Panchromatic	0.52–0.90	15
Landsat-8 OLI &TIRS (Operational Land Imager) & (Thermal Infrared Sensor)	Band 1—Ultra Blue	0.435–0.451	30
	Band 2—Blue	0.452–0.512	30
	Band 3—Green	0.533–0.590	30
	Band 4—Red	0.636–0.673	30
	Band 5—Near Infrared (NIR)	0.851–0.879	30
	Band 6—Shortwave Infrared (SWIR) 1	1.566–1.651	30
	Band 7—Shortwave Infrared (SWIR) 2	2.107–2.294	30
	Band 8—Panchromatic	0.503–0.676	30
	Band 9—Cirrus	1.363–1.384	30
	Band 10—Thermal Infrared (TIRS) 1	10.60–11.19	100* (30)
	Band 11—Thermal Infrared (TIRS) 2	11.50–12.51	100* (30

*TM Band 6, ETM + Band 6 and OLI Band 10, 11 are acquired at 120 m, 60 m and 100 m, respectively, but products are resampled to 30 m pixels. (Source: USGS)

Annex 2: Confusion Matrix of LULC Classification Map of 1991, 2006 & 2021

A

Land Class Name		Reference Data_1991					Row Total	User's accuracy (%)
		Agricultural L	Builtup Area	Bare Land	Forest Land	Grass Land		
Classified Data_1991	Agricultural L	73	0	0	4	3	**80**	91.25
	Built-up Area	0	45	3	0	1	**49**	91.84
	Bare Land	0	5	26	0	0	**31**	83.87
	Forest Land	4	0	0	47	0	**51**	92.16
	Grass Land	2	1	1	0	32	**36**	88.89
Column Total		**79**	**51**	**30**	**51**	**36**	**247**	
Producer's accuracy (%)		*92.41*	*88.24*	*86.67*	*92.16*	*88.89*		

Overall Accuracy (%) = 90.2

Kappa Coefficient = 0.874

B

Land Class Name		Reference Data_2006					Row Total	User's accuracy (%)
		Agricul-tural L	Builtup Area	Bare Land	Forest Land	Grass Land		
Classified Data_2006	Agricultural L	65		0	4	5	**74**	87.84
	Built-up Area	0	49	5	0	0	**54**	90.74
	Bare Land	1	4	37	0	0	**42**	88.10
	Forest Land	4	0	0	40	0	**44**	90.91
	Grass Land	3	0	0	1	29	**33**	87.88
Column Total		**73**	**53**	**42**	**45**	**34**	**247**	
Producer's accuracy (%)		*89.04*	*92.45*	*88.10*	*88.89*	*85.29*		

Overall Accuracy (%) = 88.6

Kappa Coefficient = 0.863

C

Land Class Name		Reference Data_2021					Row Total	User's accuracy (%)
		Agricultural L	Builtup Area	Bare Land	Forest Land	Grass Land		
Classified Data_2021	Agricultural L	62	0	0	4	3	**69**	89.86
	Builtup Area	0	57	5	0	0	**62**	91.94
	Bare Land	0	4	45	0	0	**49**	91.84
	Forest Land	3	0	0	36	0	**39**	92.31
	Grass Land	3	0	0	0	25	**28**	89.29
Column Total		**68**	**61**	**50**	**40**	**28**	**247**	
Producer's accuracy (%)		*91.18*	*93.44*	*90.00*	*90.00*	*89.29*		

Overall Accuracy (%) *= 91.1*

Kappa Coefficient *= 0.893*

Annex 3: Contour Map of Woliso Area and its Surroundings District

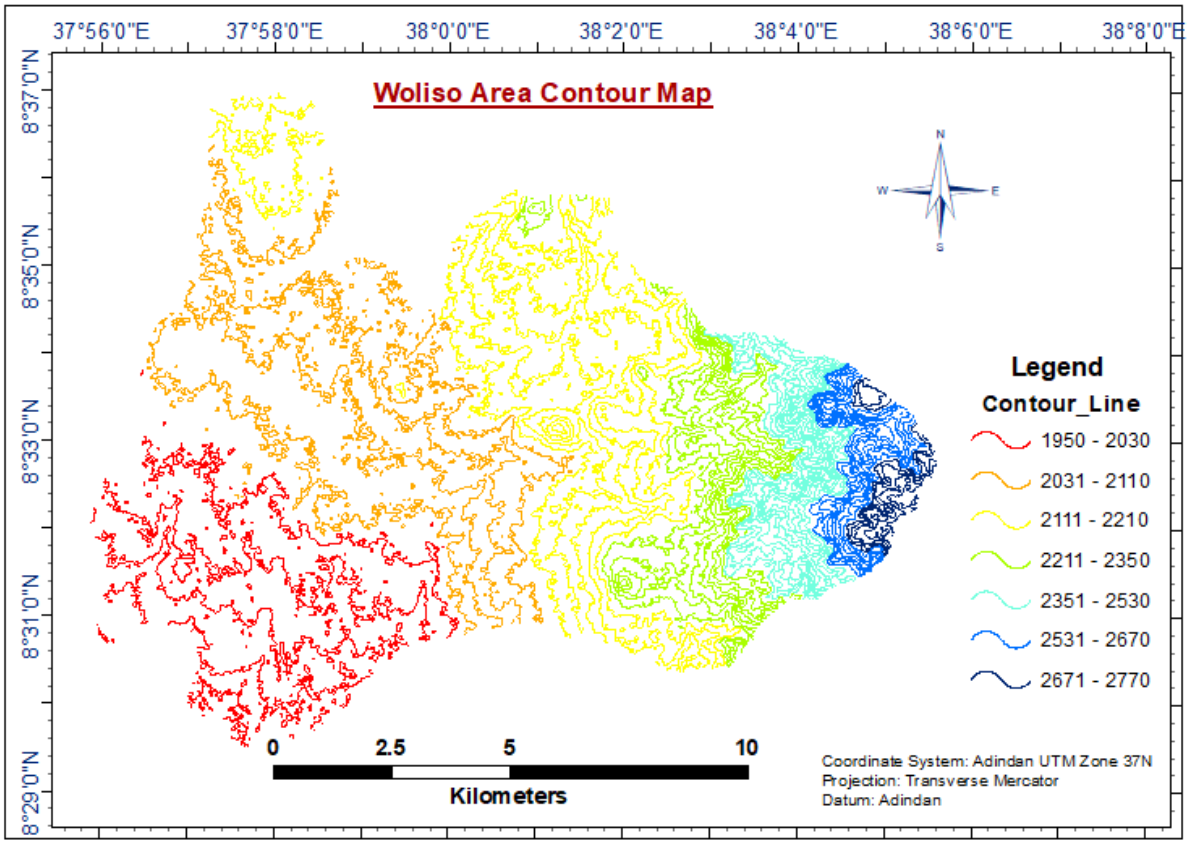

Annex 4: NDBI Maps of 1991, 1996, 2001, 2006, 2011, 2016 and 2021 Woliso

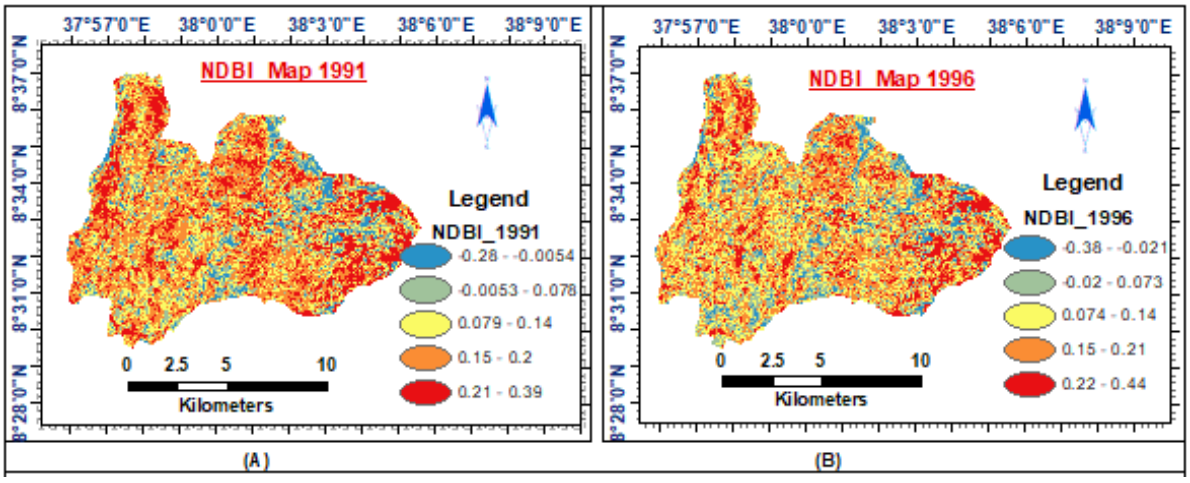

c

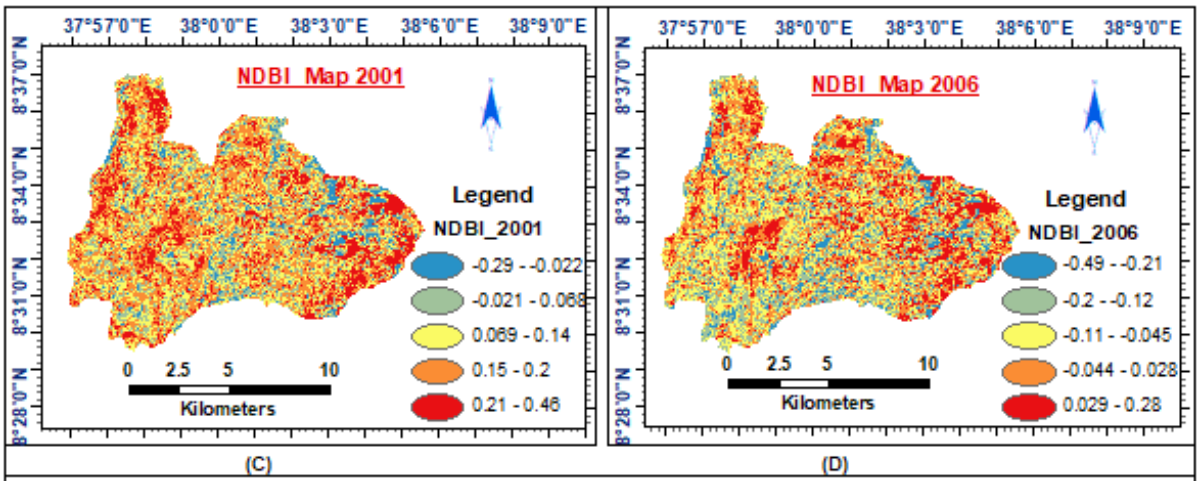

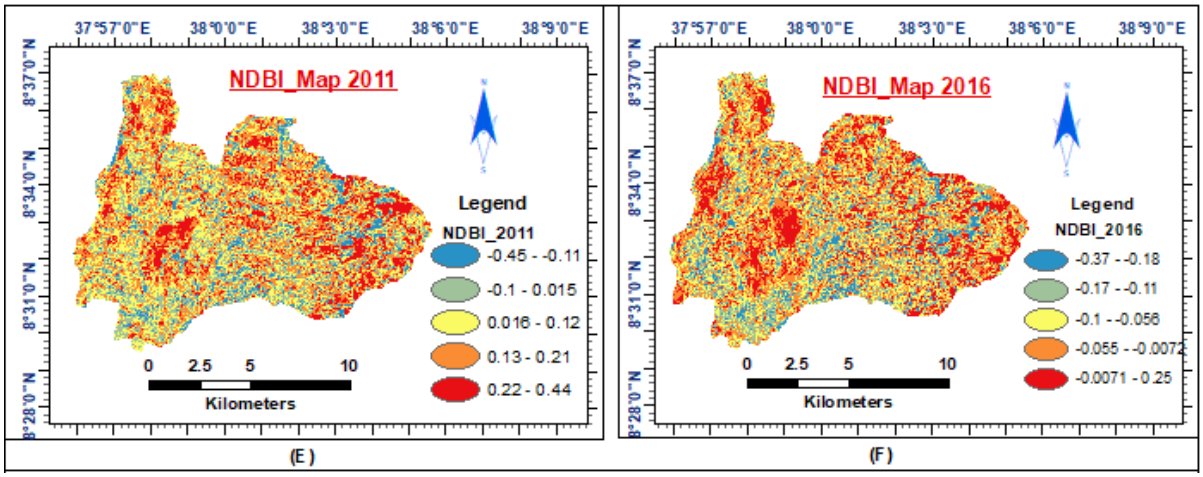

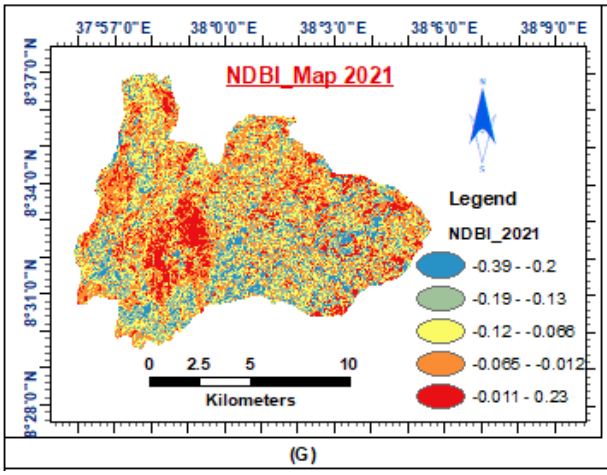

For all the Maps from (A) to (G) :

Coordinate System: Adindan UTM Zone 37N
Projection: Transverse Mercator
Datum: Adindan

d

Annex 5: Interview Guide Questions for Key Informants

Introduction

Good morning/ after noon, Dear

My name is Fikadu Fitesa and I am a post graduate student of GIS and Remote Sensing at Jimma University. Currently, I carry out academic research aimed at the impact of urban sprawl on farmlands surrounding Woliso town. The target population for this study is household heads in the study area. The result of the study will give insight about the impacts of urban sprawl on farmlands surrounding Woliso town. The participation in the discussion and interviewing process is on voluntary basis. The study is for academic purpose as a partial fulfillment for the requirement of MSc Degree and the information you provide is strictly confidential and will be used anonymously in my thesis document.

Thanks for cooperation.

1. Name of the Respondent _____, occupation _____, position if any, _____
2. District (Kebele_____), Got (Gooxii) _____
3. 3. Age ____, Educational level _____,
4. How long did you reside or serve here_____?
5. What do you witness about the process of expansion of Woliso town to the surrounding rural areas?
6. What do you think are the factors that contributed for rapid expansion of Woliso town during the last 30 years?
7. What is your view about the positive impacts of urban expansion on social, economic and environment?
8. What is your view about the negative impacts of urban expansion on social, economic and environment?
9. What do you think the government should do to improve the life of the local people affected by expansion? In capacity building, social organization, and strengthen the available institutions.
   - ✓ Things need to be introduced or avoided, Immediate need, Need for future intervention
10. What are the solutions you propose for the challenge faced as a result of expansion of the town?

Annex 6: Guide Questions for Focus Group Discussion

1. How do you see about the process of expansion of Woliso town to the surrounding rural areas and what factors contributed for rapid expansion during the last 30 years?
2. What are the positive and negative impacts of urban expansion on social, economic and environment?
3. What should be done to improve the life of the local people affected by expansion? In capacity building, social organization, and strengthen the available institutions by the government. Things need to be introduced or avoided, Immediate need, Need for future intervention
4. What are the solutions you propose for the challenge faced as a result of expansion of the town?